Dynamic modeling of HuR pathway in renal proximal tubule cells: potential induction in Renal Cell Carcinoma

By

Anoosha Sehar

NUST201260248MRCMS64012F

A THESIS SUBMITTED IN PARTIAL FULFILLMENT

OF THE REQUIREMENTS FOR THE DEGREE OF

MASTER OF SCIENCE

in

Computational Science and Engineering

RESEARCH CENTER FOR MODELING & SIMULATION

(RCMS)

National University of Sciences and Technology (NUST), Pakistan

DEDICATED TO MY BELOVED PARENTS

Declaration

I hereby declare that the work presented in the this thesis is my own effort, except where otherwise acknowledged, and that the thesis is my own composition. No part of the thesis has been previously presented for any other degree.

Anoosha Sehar

Acknowledgments

I would firstly like to express my gratefulness to Almighty Allah who gave me an opportunity to explore my natural abilitie to study computational sciences and blessed me with the courage to complete this desired task in the required time frame. All the reverence and esteem for His beloved Prophet Hazrat Muhammad (Peace Be Upon Him) the most perfect and exalted among and of born on the surface of earth, who enlightened the mankind on the true path of life and is a source of inspiration for all knowledge seekers.

My special thanks goes to my supervisor, Dr. Jamil Ahmad, Assistant Professor, RCMS, NUST, who did his level best to equip me with the latest knowledge and motivated me to move ahead to brightened the future of our country. I owe my deep gratitude to my respected committee member, Dr. Rumeza Hanif, Assistant Professor, ASAB, NUST, Islamabad, her generous and expert guidance, keen interest at every step and continuous encouragement throughout my entire research work enabled me to achieve my goals. I have a great deal of regard for my thesis committee members, Assistant professor Tariq Saeed, RCMS, NUST, Dr. Fouzia Malik, Assistant Professor, RCMS, NUST and Dr. Amjad Ali, ASAB, NUST.

I am also thankful to my colleagues who helped me come out of the difficulties I faced during the project. Due to their munificent attention, intelligence and continuous help I accomplished it within due course time. I would also like to acknowledge National University of Sciences and Technology, Islamabad for providing us the platform to undertake this research work and accomplish it within due course time.

Abstract

HuR, an RNA binding factor, is a widely expressed regulator of many cellular mRNAs at both transcriptional and post-transcriptional level. The over-expression of HuR is known to favor the progression of different types of cancers including RCC. Discrete modeling, based on the kinetic logic formalism has gained acknowledgment in the study of the interaction of genes and their Biological Regulatory Networks (BRNs). The approach helps to analyze a BRN precisely and make predictions about behaviors associated with normal or diseased conditions. In this study, we model the HuR associated BRN with the discrete modeling approach of René Thomas. The logical parameters for the model are inferred with model-checking approach implemented in the tool SMBioNet. The qualitative model predicts cyclic and stable state behaviors. Cycles represent the homeostasis of all the entities in the BRN. The stable states show the over-expression of all the proteins (AKT, HuR, NF-kB and GRB10) which can potentially lead towards Renal Cell carcinoma (RCC) while the loss of expression level will mediate the system towards apoptosis which is predicted in the second stable state where all the entities are down regulated. Additionally, the discrete model is converted into a hybrid model by incorporating clocks and delays in order to predict conditions in the form of constraints pertaining to homeostatic trajectories. The most significant delay constraint which is common in every cycle, suggests that while designing drugs for RCC the degradation rate of GRB10 must be kept higher than the activation rate of NF-κB. Suppression of GRB10 can reduce the constitutive activation of this pathway in RCC. Thus our findings suggest that GRB10 may be an attractive remedial target

in the HuR associated pathway for the therapeutic interventions against RCC.

Contents

List of Figures

List of Tables

Acronyms

AKT Serine/threonine kinase

Bio-LHA Parametric Biological Linear Hybrid Autotmata

BRN Biological Regulatory Network

CDK Cyclin-dependent kinases

CcRCC Clear cell renal cell carcinoma

ChRCC Chromophobe renal cell carcinoma

CTL Computational tree logic

GRB10 Human Growth factor receptor-bound protein 10

HuR Human Antigen R

HyTech The Hybrid Technology tool

PARA Parametrization

PDK 3-phosphoinositide-dependent kinase

PI3K phosphatidylinositol 3-kinase

PIP2 phosphatidylinositol-bisphosphates

PIP3 phosphatidylinositol-trisphosphates

RCC Renal Cell Carcinoma

RTK Receptor Tyrosine Kinases

SMBioNet Selection of Models of Biological Networks

Part I

Introduction

Chapter 1

Introduction

Cancer is rapidly becoming a worldwide pandemic as it causes 1 in 8 deaths globally [1]. According to the International Agency for Research on Cancer, there were 12.7 million new cancer cases in 2008 and with the same rate, the global cancer burden is expected to nearly double to 21.4 million cases and can result in 13.5 million deaths by 2030 [1]. Pakistan has a major cancer burden and increasing tendency of risk factors, it is a nation in dire need of cancer control.

Kidney cancer is the most deadly urologic cancer and the primary cause of cancer deaths which is ranked at sixth position in the developed nations [2]. The most common type of kidney cancer is Renal Cell Carcinoma (RCC) also termed as Renal Cell Adenocarcinoma or Renal Cell Cancer. Almost 9 out of 10 cases of kidney cancers are usually RCC [3]. RCC generally grows as a solitary or multiple tumors in a single or both kidneys. RCC is only engaged to the region of renal pelvis or renal medulla which makes it distinct from kidney cancer and it only applies to the cancer that forms in the lining of the kidney bed (i.e. in the renal tubules) [4]. It is considered as a challenging disease regardless of the enormous efforts in latest years to come up with an efficient treatment. The best likelihood of therapy lies in the early recognition of the infection when the cancer is organ-confined and hence opens for radical surgical removal [5]. The present study will pave the way for possible prospects to modify the cure for renal

cancer patients in the upcoming days.

1.1 Role of the Human Antigen R in RCC

Human antigen R (HuR) is the first RNA Binding Protein that is revealed to play a significant role in carcinogenesis and cancer progression. HuR increases the stability and elevate the intensity level of many cyclins which trigger CDK's at different cell cycle points which subsequently increase the tumor mass [6]. Many human malignancies are reported to be caused due to over-expression of HuR including renal cancer, gastric cancer, breast cancer, ovarian tumor and skin carcinoma [7].

Experimental data suggest that over-expression of HuR is significantly associated with the particular clinicopathological features, advanced stage, and poor survival in patients of RCC [7]. Several targets of HuR reported in previous studies are involved in RCC. The HuR protein binds to the mRNA of Cyclooxygenase (COX-2) and shuttle from nucleus to the cytoplasm, where it stabilizes the COX-2 mRNA. Previous findings reveal that knockdown of HuR using siRNA also reduced the expression level of COX-2 [8]. The expression of COX-2 was shown to be linked with an advanced stage of RCC and other clinicopathological features such as tumor size and grade. In addition to COX-2, HuR can also regulate the expression level of parathyroid hormone-related protein (PTHrP) protein by binding its mRNA. HuR knock down also decreases the expression of PTHrP [8, 9]. Inhibition of PTHrP leads to cell death in RCC, and comes out to be one of the important prognostic factors in the treatment of RCC [10]. Over-expression of HuR also increases the expression of Vascular Endothelial Growth Factor (VEGF) protein in hypoxic cells by stabilizing VEGF mRNA [8]. Therefore, studies confirmed that the pathological over-expression of HuR by just a few folds can lead to tumorigenicity while the loss of HuR expression induces immediate cell death, thus the regulation of HuR expression must be very tightly controlled in biological systems.

1.2 Problem Statement

HuR has been considered as a major therapeutic target in RCC for scientists. In the current study, we are interested in finding out the role of HuR abberant expression in mediating renal cancer when it binds the mRNA of Human Growth factor receptor-bound protein 10 (GRB10) and positively regulates its expression [11]. GRB10 stimulates the functioning of serine/threonine kinase AKT by translocating it to the plasma membrane, where AKT is phosphorylated and activated by the enzyme phosphatidylinositol 3-kinase PI3K [12]. AKT activates Nuclear Factor Kappa B (NF-κB), which regulates HuR transcription [11]. In this way HuR carries out a vital role in cell survival by increasing AKT signaling in a positive feedback loop. Over-expression of HuR in this signaling pathway may potentially lead towards RCC. Therefore, by modeling this pathway with formal approaches, we can analyze the dynamics of HuR expressions along with the expression of other entities of this pathway in order to identify targets for drugs in RCC. Targeting this pathway or one of its downstream target genes, particular for RCC, may thus constitute future targets for therapeutic intervention. Thus, the modeling and analysis of HuR associated pathway can help in identifying suitable targets which can appear as a promising preference to improve the efficacy of novel anti-cancer therapies against RCC.

1.3 Theme of the Study

The primary theme of the study is the use of logical approach introduced by René Thomas which is utilized to study HuR associated pathway in RCC. The study also use the model checking approaches to infer logical parameters of HuR associated Biological Regulatory Network (BRN) of the pathway satisfying the biological observations. Discrete modeling helps to observe and analyze the qualitative behavior of the BRN particularly, homeostasis (cycles) and stable states. Computational approaches

from network biology are utilized for more in-depth analysis of network. Additionally, discrete model is transformed into a hybrid model in HyTech by incorporating time delays for activation and inhibition to analyze the conditions in the form of delay constraints characterizing homeostasis. The modeling process is illustrated with a toy example of BRN.

1.4 Organization of the Thesis

The thesis starts with the extensive knowledge and background of the proteins involved in HuR associated pathway in Chapter 2. Then, all the computational approaches used in this study are described in Chapter 3. The results acquired by using the modeling and analysis approaches for the HuR related BRN are illustrated in the Chapter 4 along with the discussion based on the biological significance of the obtained results. Finally, Chapter 5 concludes this thesis.

Chapter 2

Literature Review

2.1 Epidemiology and Risk Factors for RCC

Renal Cell Carcinoma (RCC) is the most fatal of all the urologic malignancies[3, 13]. RCC accounts for 2-3% of all cancer cases and causes about 100,000 deaths worldwide annually [14]. RCC is estimated to account for 90-95% of neoplasms which occur in the kidney and cause around 3% of adult sarcomas [15]. The average frequency of RCC in men is estimated to be 12 in 100,000 while in women is 5 in 100,000. [14]. It is the ninth most common cancer in women and seventh most in men [16]. RCC is not a solitary cancer but a collection of many types of tumors with different histological subtypes [17]. It can grow as either familial (inherited), or sporadic (non-inherited) forms, and both can be related with different chromosomal genetic mutations. There are sixteen types of RCC, out of which six are grouped under familial disorders, while ten under sporadic forms [18].

Renal cancer is usually asymptotic until the late stages of the cancer. More than 50% of RCC cases are detected incidentally by using non-invasive imaging to investigate the variety of nonspecific symptoms [19]. The major symptoms of RCC includes blood in the urine of patient, flanked pain [20], fever, fatigue, weight loss and swelling in the legs and ankles. Certain types of renal tumors and cancer treatments have been

shown to cause hypertension. Users of diuretics and other anti-hypertensive medications also are associated with an increased risk of RCC. Excess body weight has been accounted for over 40% RCC cases in the US and over 30% in Europe [21]. Moreover, cigarette smoking is also hypothesized to elevate RCC cases through chronic tissue hypoxia due to carbon monoxide exposure which can play significant role in DNA damage. Chronic renal failure, radiation exposure and regular use of tobacco also contribute towards the increasing risk of RCC.

2.2 Types of RCC

RCC is divided in to four distinct subtypes. The different types of RCC are generally distinguished by the way that cancer appear when viewed under a microscope.

1. **Clear Cell Renal Cell Carcinoma**

   The most common histological and familiar sporadic subtype is Clear cell renal cell carcinoma (CcRCC) [22, 23]. It usually arises from the proximal tubular epithelium in renal cortex and is differentiated by a distinct granular or clear cell appearance. As the lipid- and glycogen-rich cells seems clear on eosin and hematoxylin staining so during histological preparations the high lipid content is dissolved in cytoplasm which leaves a clear cytoplasm that is why it is termed as clear renal cell carcinoma [24]. CcRCC comprises greater than 80% of all subtypes of RCC. [25].

2. **Papillary Renal Cell Carcinoma**

   The second most common subtype of RCC is Papillary Renal Cell Carcinoma. Papillary RCC begin from the distal tubular epithelium [26] and it accounts for 10-15% of all renal malignancies. Due to its tubulo-papillary and predominantly papillary structural design, it was separated from the category of other renal cell carcinomas.

3. **Chromophobe Renal Cell Carcinoma**

   Chromophobe Renal Cell Carcinoma (ChRCC) is another type of RCC. The incidence of ChRCC is similar in both men and women. At stage 1 or 2, nearly 86% of all the ChRCCs cases are estimated to be diagnosed. ChRCC has better prognosis than other forms of RCC. The prevalence of metastatic illness is 6-7% in ChRCC while about 5% of cases comprises of renal vein invasion. The median tumor size is larger than any other type of RCC which is predicted to be almost 6.0 cm [27]. It contains prominent cell membrane with outsized multilateral cells. Cytoplasm is whitish and resistant to staining with eosin and hematoxylin. The tumor blood vessels have substantial walls and are eccentrically hyalinized [28].

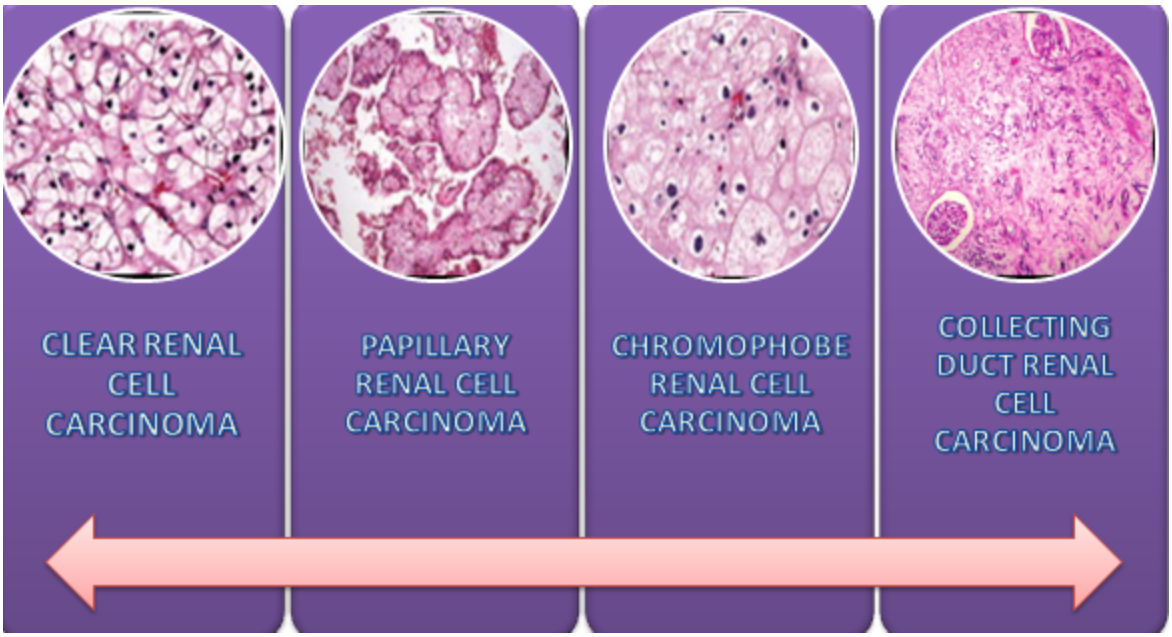

Figure 2.1: **Macroscopic view of subtypes of renal cell carcinoma:** (a) Clear cell renal carcinoma contains alveolar arrangement of cells with clear cytoplasm and nested tumor cells. (b) Papillary renal cell carcinoma have variable proportion of tubules and papillae. (c) Chromophobe renal cell carcinoma have granulated cytoplasm and have tight intracellular cohesion with distinct cell borders [29]. (d) Collecting duct renal cell carcinoma exhibits tubulo-papillary architecture with undefined bounds and prominent nuclei [30].

4. **Collecting Duct Renal Cell Carcinoma**

Collecting Duct Carcinoma (CDC) starts from the epithelium of the collecting ducts. Almost 1% of total kidney cases are comprised of CDC. Prognosis of patient depends on well defined gross and microscopic criterion [26].

2.3 Influence of the RNA Binding Protein HuR in RCC

Human antigen R (HuR) belongs to the ELAV like Hu- protein family of RNA Binding Proteins (RBPs) [31, 32], which is revealed to play a significant role in the progression of RCC [33]. It can either function as tumor suppressor or as an oncogene by regulating the expression of different target genes [7]. Experimental data suggests that HuR over-expression is significantly associated with the particular clinicopathological features, advanced stage, and poor survival in patients of RCC [7]. It is identified that intracellular HuR is mostly confined to a small area within the nucleus of resting cells. Under various environmental factors such as heat shock, energy depletion or ultraviolet radiations etc, HuR-mRNA complex is translocated to the cytoplasm [11]. After carrying out the process of stabilization, HuR detaches itself from the mRNA and returns quickly to the nucleus . This translocation from the nucleus to the cytoplasm comes out to be an essential aspect of HuR role in stabilization. But the majority of the exogenous stimuli result in an extensively increased cytoplasmic accumulation of HuR protein [7]. Apart from HuRś role as an mRNA stability protein, elevated levels of cytoplasmic HuR have been found in many types of cancers [7]. The present study is carried out to illustrate the intracellular pathway involved in RCC carcinogenicity and to identify molecular targets that might be used to design proficient, targeted, and protected therapies for this refractory disease.

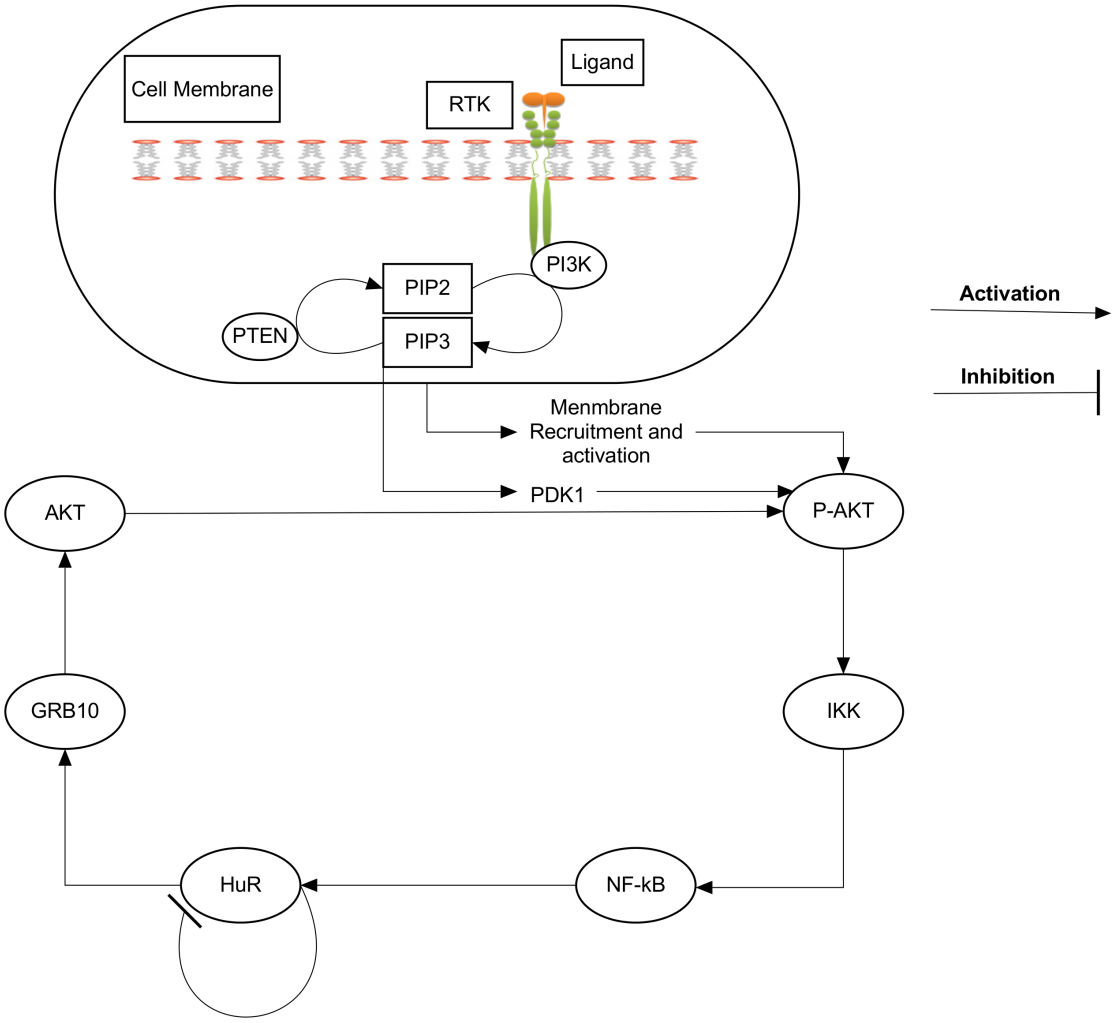

Figure 2.2: **Signaling pathway involving HuR:** One of the major intracellular signaling pathways responsible for promoting cell survival is initiated by the enzyme PI3K, which is activated by either Receptor Tyrosine Kinases (RTK) or G protein-coupled receptors (GPCR's). PI3K phosphorylates the membrane phospholipid PIP2 to form PIP3, which activates AKT, a serine/threonine kinase. PIP3 recruits the protein kinase AKT to the plasma membrane where it is activated as a result of phosphorylation by PDK. AKT then phosphorylates a number of proteins that contribute to cell survival [34].

2.4 Signaling pathway involving HuR

Previous studies have suggested interaction between HuR function and serine/threonine kinase AKT (also known as protein kinase B\PKB) signaling [35]. This signalling is initiated by the enzyme phosphatidylinositol 3-kinase (PI3K), which is activated by either receptor tyrosine kinases (RTK) or G protein-coupled receptors (GPCR's). The lipid kinase PI3K phosphorylates phosphatidylinositol-bisphosphates (PIP2), generating phosphatidylinositol-trisphosphates (PIP3), which recruit the AKT and 3-phosphoinositide-dependent kinase (PDK) to the plasma membrane. Phosphorylation by PDK activates AKT. The signal branches at the level of AKT, regulating downstream proteins that control translation and transcription. During transcription, AKT affects numerous transcription factors including NF-κB transactivation potential and induce RelA/p65 phosphorylation. In Renal Tubule Cells (RTC), activation of NF-κB promotes HuR transcription, as HuR is a direct transciption target of NF-κB [35]. HuR binds to the mRNA of Human Growth factor receptor-bound protein 10 (GRB10) adapter protein and positively regulates its expression. GRB10 stimulates the functioning of AKT by translocating it to the plasma membrane, where AKT is phosphorylated and activated by PI3K, [12] thus, forming a positive feedback loop [12]. Studies indicated that GRB10 is critical for AKT activation under both normal and stressed conditions [36]. In this way HuR carries out a vital role in cell survival by increasing AKT signaling in a positive feedback loop (Figure 2.2) [7]. The effect of this positive feedback loop is increased during stress. HuR controls its expression via negative feedback loop and maintains its level at steady and comparatively low physiological levels [7, 37]. HuR is primarily cytoplasmic in trauma or stress which possibly interrupts the negative feedback loop, thus leading to increased HuR levels and potential oncogenic transformations [36]. Aberrant expression of HuR has been shown to reduce cell viability or promotion of pathological proliferation and invasiveness [38, 39]. Pathological over-expression by just a few folds can lead to carcinogenicity while the

loss of HuR expression induces immediate cell death, therefore, the regulation of HuR expression must be tightly controlled in biological systems [33, 40, 41]. These findings, therefore reveal, the control of HuR expression and elucidate its role in a key pathway that has implications not only for cell survival under stress, but also for HuR's role in promoting tumor growth [7, 11, 32, 40].

2.5 Modeling Approaches

Current advances in molecular and computational biology are useful to study the complex transcriptional regulatory networks by finding the interactions between proteins and genes [42, 43, 44, 45]. The model presented in Figure 2.3 is created by using the René Thomas [46, 47, 48] formalism for computational verification the results of *in vitro* studies and for evaluating the role of HuR aberrant expression in mediating RCC [49, 50].

In this study, we performed a formal analysis of HuR associated pathway and its downstream targets using discrete and hybrid models [51, 52]. We have analyzed the role of HuR over-expression under stress which potentially leads towards RCC. The BRN is obtained by keeping the most important entities in which we were interested and abstracting the remaining ones, provided that the behavior is preserved (Figure 2.3). We then used the modeled BRN for obtaining the logical parameters from SMBioNet [53, 54, 55]. These parameters were used in GenoTech which computed the qualitative cycles and two stable states. This approach helped us to study a BRN and to make predictions about those steady states which lead to normal or diseased conditions. Additionally we transformed the discrete model into a hybrid model [56, 57] in HyTech [58] by incorporating time delays for activation and inhibition [59]. The computation of convergence domain enabled us to observe the parametric constraints governing the oscillatory behavior of all proteins. Through the relation matrices of the trajectories [60], we extracted the most significant pair wise constraints, the violation

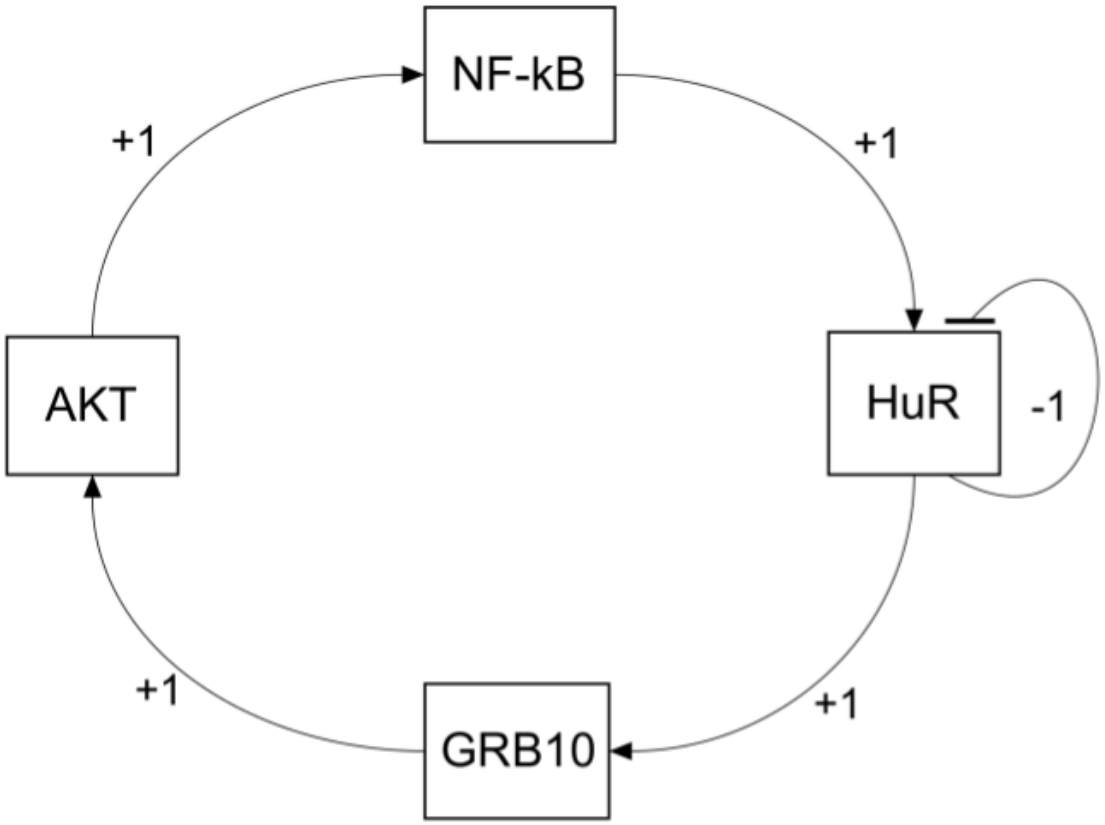

Figure 2.3: **HuR associated BRN:** AKT activation stimulates NF-κB activity, which promotes HuR transcription. HuR binds to the adapter protein GRB10 and regulates its expression. GRB10 facilitates the translocation of AKT to plasma membrane where PI3K phosphorylates and activates AKT by forming a positive feedback loop [12]. The model has been reduced by implicit modeling of involved entities whilst keeping their behavior preserved. Thresholds are given positive and negative signs. Positive sign represents activation while negative signifies inhibition. [11, 34, 36].

of which will interrupt the cyclic behavior and diverge the system towards either of the stable state. Our study suggests that all proteins showed oscillatory behavior in the system and will maintain their expression. HuR shuttles from the nucleus to the cytoplasm under cellular stress, where there is a chance that its auto-regulatory behavior gets interrupted leading to its uncontrolled transcription [36]. Our analysis verified that the over-expression of all entities plays a pivotal role in mediating renal cancer while the loss of expression will mediate apoptosis [11, 36, 61]. The most important prediction based on the analysis of hybrid model is that the rate of degradation of

GRB10 is higher than the activation rate of NF-κB in all the cycles representing the homeostasis of entities particularly HuR. Previously it was reported that NF-κB and HuR maybe targeted for drugs against RCC [8, 62, 63]. Since NF-κB is involved in many important cellular activities and HuR oscillation is vital against RCC. Therefore we suggest that GRB10 maybe a better target as compared to NF-κB and HuR. These findings suggest that novel therapy should target GRB10 i.e. inhibitor should be identified or designed to suppress GRB10.

Part II

Modeling and Analysis

Chapter 3

Methodology

The essential biological systems can be represented in the form of networks which provide a backbone for dynamic modeling and structural analysis [64]. Structural analysis incorporates the use of graph-theoretic measures to obtain information on the organization of the network where as the dynamic models reveal the fact that the vertices of the network are molecular species, and also illustrate that how the population level of these species alter over time [47].

3.1 Biological Regulatory network (BRN)

Current advances in computational biology have made achievable the study of complex biological networks [65] that explain gene expression precisely by interactions between proteins and DNA. Biological Regulatory Network (BRN) is the illustration of multiple interactions inside a cell, it helps us to understand the relationship between cellular entities [66]. The components of the BRN composed of nodes and edges. The nodes of the BRN mainly consist of genes, proteins and mRNAs while the edges indicate the interactions between nodes. The activation of an entity is shown by a positive sign whereas inhibition is represented by a negative sign. We can deal with enormously complex and advanced biological networks by knowing about the components existing

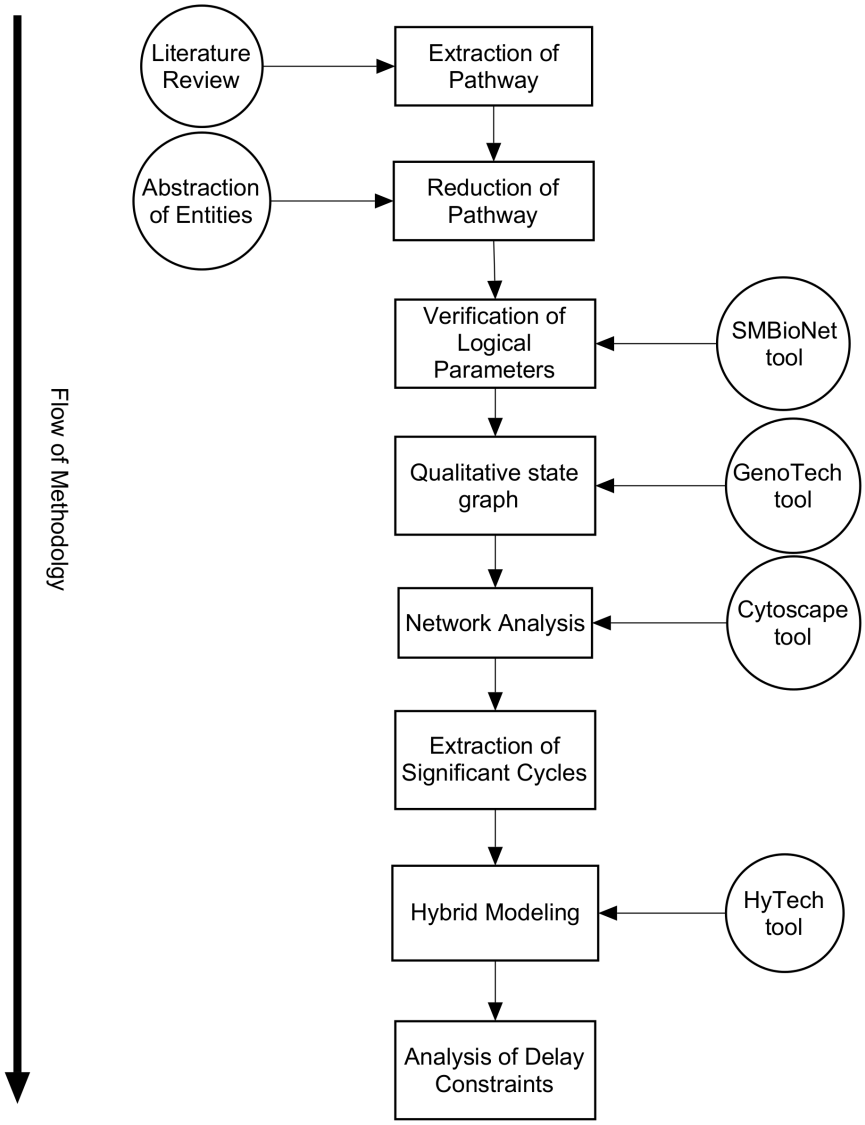

Figure 3.1: The methodology employed to the model for the analysis of HuR associated BRN

.

within a cell. Formal approaches can be used to model and analyze the behavior of the entities involved in the BRN.

3.2 René Thomas Approach

In 1970s, René Thomas presented a Boolean approach for biological systems in which the expression of the entities such as genes and proteins were declared as on or off. This approach was used to depict the qualitative nature of the entities, where the evolution of entities were represented by a state transition graph [46, 47, 48, 67]. Later on, René Thomas expanded it up to the multivalued levels of fixation and named it as "Kinetic logic". BRNs have a significant role in all life processes such as cell cycle regulation, cell differentiation, and metabolism [68]. Any interruption in these cellular processes can lead to different diseases, the mechanism of which can be studied by understanding the dynamics of BRN.

3.2.1 Semantics of René Thomas Formalism

The Semantics of René Thomas formalism [60, 69] are shown by a dummy example of BRN which comprises of three entities n_1, n_2 and n_3 as shown in Figure 3.2.

Definition 1 (Directed Graph)**.** *A directed graph G is a tuple <V, E >where V is a set of vertices and* $E \subseteq V \times V$ *is a set of edges.*

The set of vertices and edges for the directed graph in Figure 3.2 are $\{n_1, n_2, n_3\}$ and $\{(n_1, n_2), (n_2, n_3), (n_3, n_1)\}$ respectively. In graph G=(V,E), $G^-(n)$ and G^+(n) represent the predecessors and successors of a vertex n $\in$ V, respectively. (n_1, n_2) is an edge which is directed from $n_1 \rightarrow n_2$, where n_2 is known to be its head and n_1 is called as tail. $G^-(n_1) = \{n_3\}$ and $G^+(n_1) = \{n_2\}$ denote the set of predecessors and successors of a vertex $n_1 \in$ V, respectively.

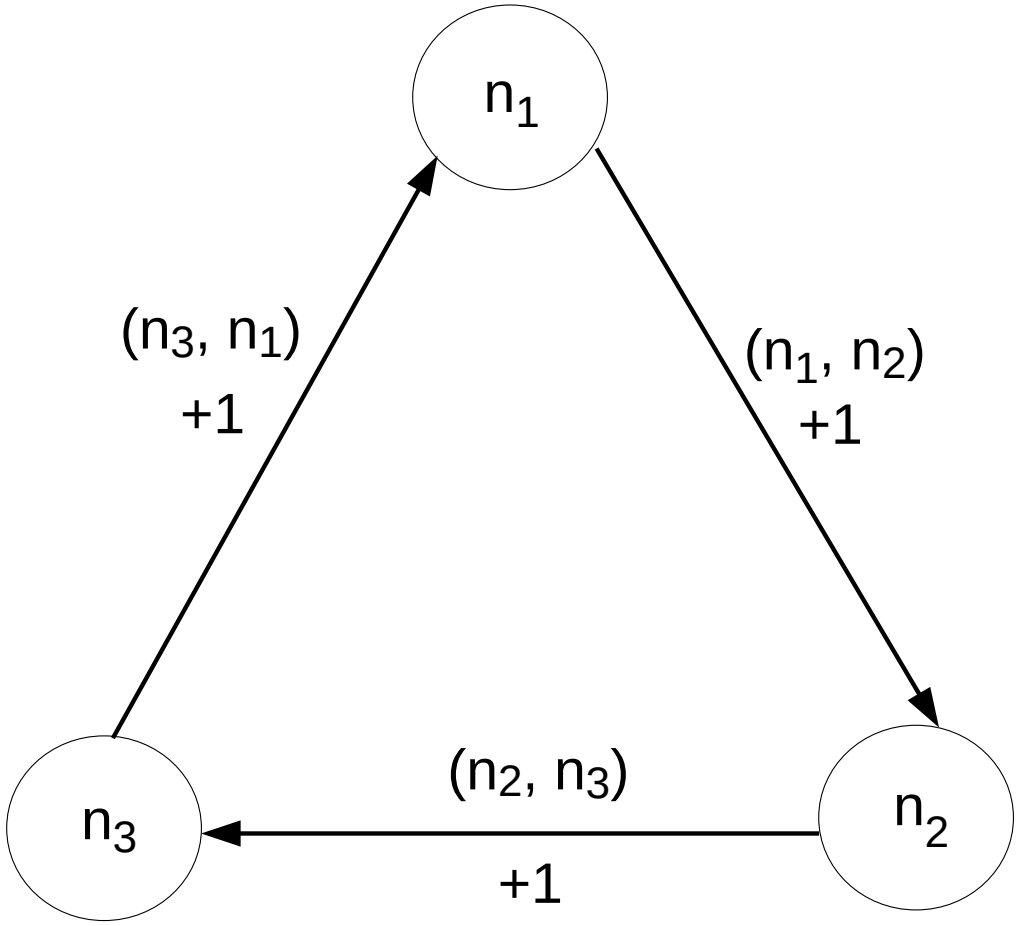

Figure 3.2: **Toy example of a BRN:** Entities are labeled as n_1, n_2 and n_3. (n_1, n_2), (n_2, n_3), (n_3, n_1) represents the direction of edges, whereas 1 indicates the threshold level with a positive sign representing activation of the entity.

Definition 2 (Biological Regulatory Network (BRN))**.** *A Biological Regulatory Network (BRN) is a labeled directed graph G=(V,E), where set of vertices V represents biological entities, and* $E \subseteq V \times V$ *represents the interaction between entities. Every edge* $n_i \rightarrow n_j$ *is labeled by a pair* $(f_{n_i n_j}, \alpha_{n_i n_j})$*, where* $f_{n_i n_j}$ *is a positive number for representing a qualitative threshold and* $\alpha_{n_i n_j}$ *is either a (+) sign for activation or a (-) sign for deactivation of an entity.*

- *Each vertex* n_i *has a limit* u_{n_i} *which represents the total number of targets of* n_i *and is equal to out-degree of* n_i*, such that* $u_{n_i} = |G^+_{(n_i)}|$.

- *Set* $W_{n_i} = \{0, 1 \cdots, r_{n_i}\}$ *of an entity* n_i *represents the qualitative concentration levels where* $r_{n_i} = max\{f_{n_i.n_k} | n_k \in G^+(n_i)\}$.

Definition 3 (States)**.** *The qualitative state* $s \in S$ *of a BRN, G =(V,E), is a tuple representing the qualitative expression level of all biological entities and the set of states can be expressed as* $S = \Pi_{n_i \in V} W_{n_i}$*. The states are qualitatively characterized by vector* $(s_{n_i})_{\forall n_i \in V}$*, where concentration level of product* n_i *is indicated by* s_{n_i}*. A qualitative state signifies a relationship of all the elements of a BRN at any instant of time. The numbers of activators of a specific variable at a particular level of concentration are indicated by its set of resources.*

Table 3.1: Table shows all the possible states, resources and logical parameters of a dummy BRN shown in Figure 3.2

s_{n_1}	s_{n_2}	s_{n_3}	$Q_{s_{n_1}}$	$Q_{s_{n_2}}$	$Q_{s_{n_3}}$	$K_{n_1}(Q_{s_{n_1}})$	$K_{n_2}(Q_{s_{n_2}})$	$K_{n_3}(Q_{s_{n_3}})$
0	0	0	{}	{}	{}	0	0	0
0	0	1	$\{n_3\}$	{}	{}	1	0	0
0	1	0	{}	{}	$\{n_2\}$	0	0	1
0	1	1	$\{n_3\}$	{}	$\{n_2\}$	1	0	1
1	0	0	{}	$\{n_1\}$	{}	0	1	0
1	0	1	$\{n_3\}$	$\{n_1\}$	{}	1	1	0
1	1	0	{}	$\{n_1\}$	$\{n_2\}$	0	1	1
1	1	1	$\{n_3\}$	$\{n_1\}$	$\{n_2\}$	1	1	1

Definition 4 (Resources)**.** *The set of resources* $Q_{s_{n_i}}$ *of an entity* $n_i \in V$ *at a level* s_{n_i} *of BRN G is defined as*

$$Q_{s_{n_i}} = \{n_j \in G^-(n_i) | (s_{n_j} \geq f_{n_j n_i} \quad and \quad \alpha_{n_j n_i} = +) \quad or \quad (s_{n_j} < f_{n_j n_i} \quad and \quad \alpha_{n_j n_i} = -)\}$$

It is to be noted that inhibitor is considered as an activator in its absence. The dynamic properties of BRN depends on logical parameters. The set of these logical parameters is illustrated as $K(G) = \{K_{n_i}(Q_{s_{n_i}}) \in W_{n_i} \ \forall \ n_i \in V\}$*. The parameter* $K_{n_i}(Q_{s_{n_i}})$

provides the information related to the evolution of n_i at particular level. It is suitable to express the transition between two qualitative states by the evolution operator $\Rsh$ [60], which is defined as follows:

$$s_{n_i} \Rsh K_{n_i}(Q_{s_{n_i}}) = \begin{cases} s_{n_i} + 1 & if s_{n_i} < K_{n_i}(Q_{s_{n_i}}); \\ s_{n_i} - 1 & if s_{n_i} > K_{n_i}(Q_{s_{n_i}}); \\ s_{n_i} & if s_{n_i} = K_{n_i}(Q_{s_{n_i}}); \end{cases}$$

Where s_{n_i} and $K_{n_i}(Q_{s_{n_i}}) \in W_{n_i}$

Definition 5 (Parametric State Graph)**.** *The concentration level of entity n_i in state s is represented by $s = (s_{n_i})_i \in S$. Then the state graph of the BRN G=(V,E) is the labeled directed graph such that G=(S,T), where S is a set of states and $T \subseteq S \times S$ represents a relation between states, known as transition relation, such that $s \to s^{'} \in T$ if and only if:*
1: $\exists$ a unique $n_i \in V$ such that $s_{n_i} \neq s^{'}_{n_i}$ and $s^{'}_{n_i} = s_{n_i} \Rsh K_{n_i}(Q_{s_{n_i}})$, and
2: $\forall\ n_j \in V \backslash \{n_i\}\ s^{'}_{n_j} = s_{n_j}$

Definition 6 (Cycle)**.** *A cycle can be defined as a closed path where the initial and terminal vertex(state) is the same.*

3.3 Model Checking

SMBioNet SMBioNet is a software which is used to find the logical parameters for the modeling of BRN. It works on the formalism of kinetic logic given by René Thomas [53, 55]. SMBioNet helps to verify systematically the coherence of models of a given biological system, and to select the suitable models which satisfy the temporal properties extracted from knowledge or hypothesis.

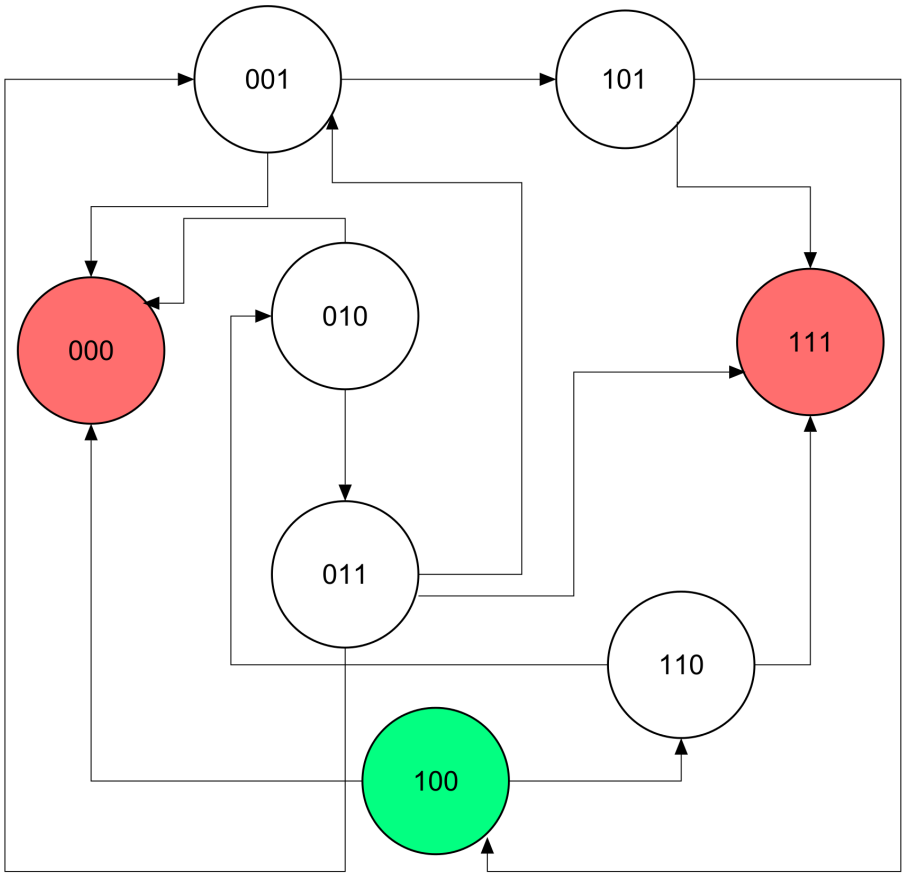

Figure 3.3: Parametric State Graph: (100) represents the starting state of dummy BRN. The states (000) and (111) are the two stable stables with no outgoing arcs.

Input The input data usually comprises of a distinct biological network in discrete form with undetermined parameters or constraints [70].

- 1 represents activation
- 0 represents deactivation

Parametrization There is a section titled PARA in which each variable is assigned some logical parameters by default, depending on the threshold value of that variable. This section confers limitations on logical parameters to take values within the range of intervals [54].

Computational tree logic Formula (CTL) The other section of the input consists of CTL formulae. The CTL formula expresses the dynamical properties and the biological observations for modeling the system [71]. The following notations are used for temporal operators.

- **E:** There **E**xists a path
- **A:** In **A**ll paths
- **F:** Sometime in the **F**uture
- **G:** **G**lobally in the future
- **X:** Ne**X**t time

The CTL formula for the dummy BRN in Figure 3.2 is as follows: ϕ_1 represents the cyclic behaviour of trajectories, while ϕ_2 and ϕ_3 represent the stable states. Finally, ϕ denotes the conjunction of the three CTL properties.

$$Init = (n_1 = 1 \quad \& \quad n_2 = 0 \quad \& \quad n_3 = 0) \tag{3.1}$$

$$Stable \quad State1 = (n_1 = 1 \quad \& \quad n_2 = 1 \quad \& \quad n_3 = 1) \tag{3.2}$$

$$Stable \quad State2 = (n_1 = 0 \quad \& \quad n_2 = 0 \quad \& \quad n_3 = 0) \tag{3.3}$$

$$\phi_1 = Init \rightarrow AX(EF(Init)) \tag{3.4}$$

$$\phi_2 = Init \rightarrow EF(AG(StableState1)) \tag{3.5}$$

$$\phi_3 = Init \rightarrow EF(AG(StableState2)) \tag{3.6}$$

$$\phi = \phi_1 \quad \& \quad \phi_2 \quad \& \quad \phi_3 \tag{3.7}$$

Output All possible logical parameter sets are obtained which obey the parametrizations of the network and satisfy the specific CTL formula. NuSMV model checker is used to check the CTL formulas while generating the logical parameters [72, 73, 74].

3.4 GenoTech

GenoTech is a tool written in java and is used for the discrete modeling of BRN. This tool has the ability to qualitatively model the complex biological networks. A regulatory network in GenoTech is represented by a directed graph where vertices represent biological entities which can be genes or proteins, and edges symbolize interactions between the entities [45]. The edges are always marked with discrete numbers which represent thresholds for certain concentration level and signs of interactions which include '+' for activation while '-' for deactivation [69].

3.5 Network analysis

Data can be represented as an intricate network for extracting the most important patterns in it [75]. An intricate network shows the interactions of entities in a complex system. The BRN usually represents protein-protein interactions in cellular processes. The intrinsic variability in biological data and the high probability of data imprecision requires incorporation of network dynamics and topology for the study of biological systems [76]. The components of a system and their relationship are best described as networks and they are mostly represented as graphs where many vertices are interconnected. In this study, we demonstrate techniques and the ways which can be

used to expose unknown properties and features of a network. After discrete modeling of the BRN, the state graph was analyzed using Cytoscape [77]. This network profiling joined with knowledge extraction facilitated us to understand the biological implication of our system [56], in particular with the relatively important trajectories than the rest of the trajectories exhibited by the system [78]. The required properties related to our study are given below [79, 80, 81]:

Definition 7 (Distance)**.** *The number of transitions that need to be traversed in order to reach from one state to the other is known as distance. The shortest distance between two states is denoted as* d_{ew} *where* $e,w \in S$.

Definition 8 (Betweenness Centrality)**.** *Betweenness Centrality shows that the state* $e \in S$ *ranked higher between its intermediary neighbor states.*

Without this state, there would be no way for two neighbors to communicate with each other. $C_{spb} = \sum_{u \neq e \neq w \in S} \frac{\sigma_{uw}(e)}{\sigma_{uw}}$ where, $\sigma_{uw}$is the total number of paths between the states u and w from the set of all shortest paths. $\sigma_{uw}(e)$ is the total number of paths between the states u and w, from the set of all shortest paths, which pass through the state e $\in$ S.

Centrality analysis is the measurement that shows whether the states of the network have the same connectivity. The lower the centralities of the states on average, the more homogenous (or less clustered) the connections are between the states. On the other hand, the higher the network centrality of particular states, the less homogenous (or more clustered) the network becomes [82]. Network centralities show how states can be placed or sorted according to their properties. It is important in biological networks to identify central or transitional states that affect the network topology [76].

3.6 Hybrid modeling

The class of hybrid modeling bridges the gap between continuous and discrete modeling. Each node is characterized by two variables, a discrete activity and a continuous concentration. In 1985, a novel modeling approach was initiated by Kaufman et. al., which considered the threshold time phase required to begin the synthesis, execution, and the degradation process [71, 83]. The choice to select the appropriate model depends upon the level of quantitative information which we get from any experimental data. Continuous models can be used when adequate kinetic details can be obtained, discrete models are best employed for systems with no kinetic information or for the less-characterized systems whereas hybrid models can be used when limited knowledge on the kinetic parameters exists [84]. A hybrid model of a BRN comprises of discrete locations coupled with continuous variables (clocks). The discrete transitions represent the immediate change between locations whereas the continuous transitions show time that elapses in a location [86]. Figure 3.5 shows the evolution of proteins in a discrete fashion (from s_{n_j} to $s_{n_{j+1}}$, or $s_{n_{j+1}}$ to s_{n_j}). However in reality, the concentration level of these proteins changes in an uninterrupted continuous manner and such activities cannot be captured using only the discrete modeling framework. Figure 3.4 shows the evolution of proteins in a continues manner. A delay is compulsory for the evolution of a protein from level s_{n_j} to $s_{n_{j+1}}$, or from $s_{n_{j+1}}$ to s_{n_j}. Towards end, the additional concept of clock variables measuring said delays were introduced [59, 86]. Clocks are continuous variables used in models based on hybrid automata and, its subclass, timed automata. A clock variable h is associated with every entity that synchronously evolves with time. The time calculated between two levels by the clock variable h is called the delay time between these two levels. Initially, the value of the clock is set to zero and when the clock value gets equivalent to delay time $\mathrm{d}^+_{n_j}$ or $\mathrm{d}^-_{n_j}$ the transition between two levels takes place. The delays $\mathrm{d}^+_{n_j}$ depicts time taken from s_{n_j} to $s_{n_{j+1}}$ which is called as positive delay or production delay. However, the time delay $\mathrm{d}^-_{n_j}$ shows tran-

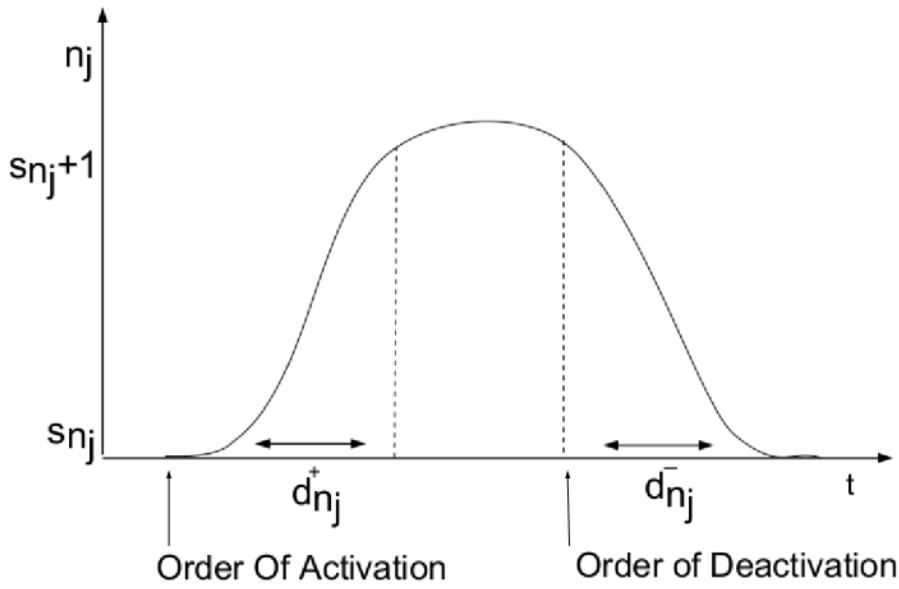

Figure 3.4: Timing diagram showing actual evolutionary path of proteins [85].

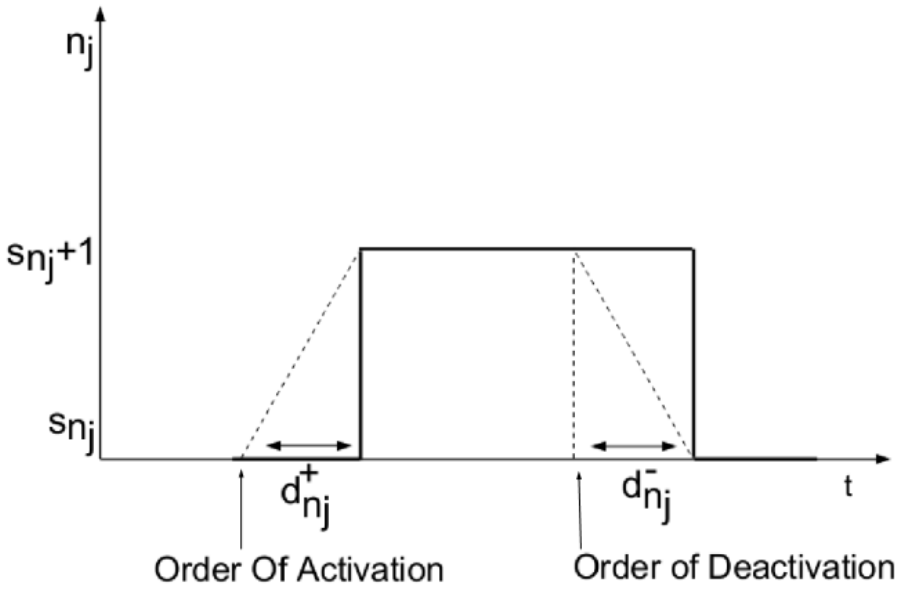

.

Figure 3.5: Evolution of proteins in discrete fashion [85].

sition from $s_{n_{j+1}}$ to s_{n_j} which is termed as negative delay or degradation delay (Figure 3.4 and 3.5) [69]. Thus, a biological linear hybrid automaton (Bio-LHA) [59, 86] is constructed (Figure 3.6) to show both the discrete and continuous timed dynamics of the system.

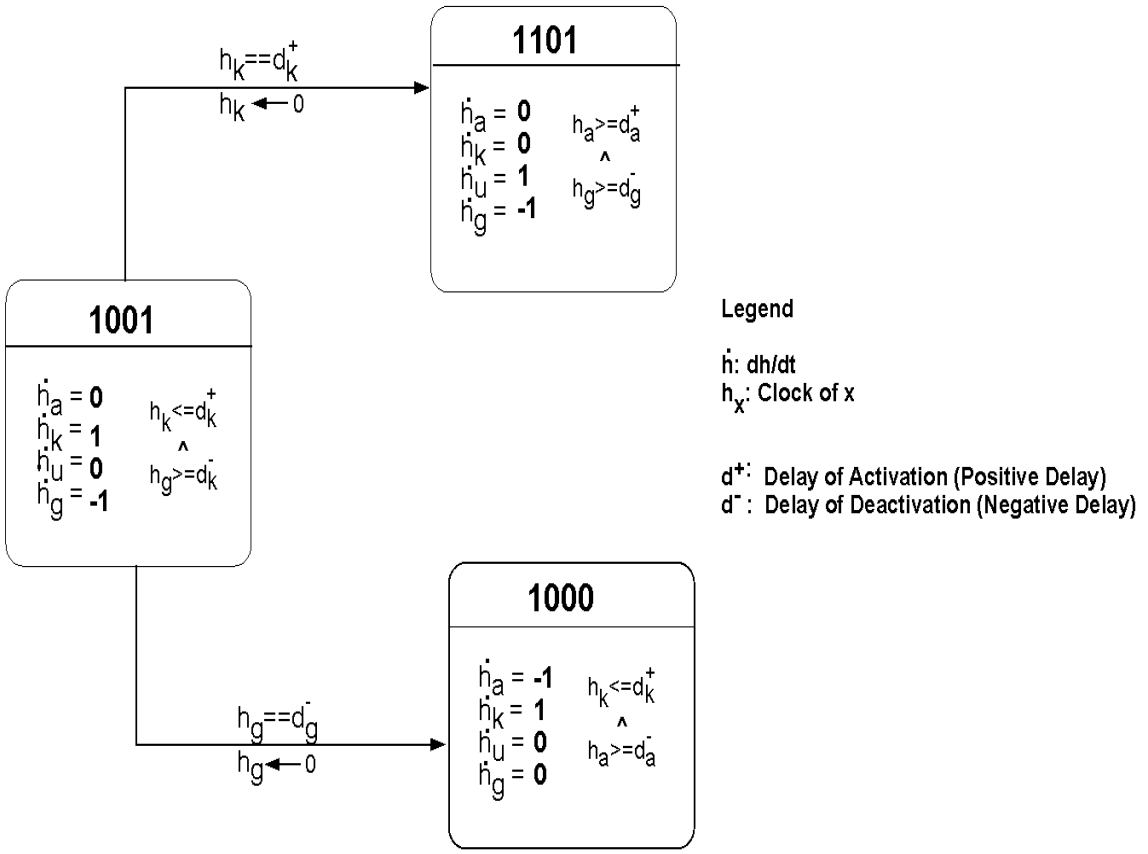

Figure 3.6: **Partial view of Bio-LHA of the HuR associated BRN.** (1001), (1101) and (1000) are the states of BRN, consisting of four entities i.e. AKT (a), NF-κB (k), HuR (u) and GRB10 (g), each transition is marked with guard. While each location is marked with entity rates and the invariants (conjuncted constraints).

"Let $C^{=}(X, P)$, $C^{\leq}(X, P)$, and $C^{\geq}(X, P)$ be the set of constraints using only $=$, $\leq$ and $\geq$, respectively. Here X and P are the sets of real valued variables and parameters, respectively.

Definition 9 (Parametric Bio Linear Hybrid Automaton (Bio-LHA))**.** *A parametric Bio linear hybrid automaton* $\mathbb{B}$ *is a tuple (I,* i_0*, X, P,* $\mathbb{E}$*, Inv, Dif) where*

- *L is a finite set of locations.*
- $l_0 \in L$ *is an initial location.*
- *P is a finite set of parameters (delays).*
- *X is a finite set real-valued variable (clocks).*
- $\mathbb{E} \subseteq L \times C^{=}(X,P) \times 2^X \times L$ *is a finite set of edges,* $e = (l, g, R, l^{'}) \in \mathbb{E}$ *represents an edge from the location l to the location* $l^{'}$ *with the guard g and the reset set* $R \subseteq X$.
- *Inv:* $L \rightarrow C^{\leq}(X,P) \cup C^{\geq}(X,P)$ *allocates an invariant to any location.*
- *Dif:* $L \times X \rightarrow \{-1, 0, 1\}$ *maps each pair (l, h) to an evolution rate.*

The semantics of a parametric Bio-LHA is a timed transition system. We labeled the semantics according the time domain $\mathbb{T}$, assuming $\mathbb{T}^* = \mathbb{T} \backslash \{0\}$.

Definition 10 (Semantics of Bio-LHA)**.** *Let* β *be a valuation for the parameters P and v which corresponds to the values of clocks in a location. The* ($\mathbb{T}$, β)*-semantics of a parametric Bio-LHA* $\mathbb{B}$= *(L,* l_0*, X, P,* $\mathbb{E}$*, Inv, Dif) is defined as a timed transition system M =(S,* s_0*,* $\mathbb{T}$*,* $\rightarrow$*) where (1)* $S = \{(l, v) \mid l \in L$ *and* $v \models Inv(l)\}$*; (2)* s_0 *is the initial state and (3) The relation* $\rightarrow \subseteq S \times \mathbb{T} \times S$ *is defined for* $t \in \mathbb{T}$ *as:*

- **Discrete Transitions** $(l,v) \rightarrow (l^{'}, v^{'})$ *iff* $\exists$ $(l, g, R, l') \in \mathbb{E}$ *such that g(v)=true,* $v^{'}(h) = 0$ *if* $h \in R$ *and* $v^{'}(h)= v(h)$ *if* $h \notin R$.
- **Continues Transitions** *For* $t \in \mathbb{T}^*$, $(l,v) \rightarrow (l^{'}, v^{'})$ *iff* $l^{'} = l$, $v^{'}(h) = v(h) + Dif(l, h) \times t$, *and for every* $t^{'} \in [0,t]$, $(v(h) + Dif\ (l,h) \times t^{'}) \models Inv(l)$, *where* $\models$ *represents satisfaction operator.*

Definition 11 (Temporal zone)**.** *Temporal zone is defined as a region where time elapses until the discrete value of one variable between two consecutive states is changed.*

Definition 12 (Temporal state space)**.** *The union of all the temporal zones obtained from discrete model of BRN is called a temporal state space.*

Definition 13 (Invariance Kernel)**.** *Let $\phi(t) \in S\ \forall t \geq 0$ be a trajectory in a temporal state space S. The biggest subset K of S is the invariance kernel if $p \in K$, a trajectory starting at point p is viable in K .*

The invariance kernel demands that all cyclic or oscillatory trajectories are completely periodic, meaning that the trajectories are not asymptotic. Conversely, a convergence domain can also be defined based on the asymptotic properties.

Definition 14 (Convergence Domain)**.** *The subset K(S) is called the convergence domain if $\forall p \in K$, the trajectory starting at point p converges in an asymptotic manner". [60, p. 284]*

Part III

Results and Discussion

Chapter 4

Results And Discussion

The results acquired by using the modeling and analysis techniques for the HuR related BRN shown in Figure 2.3 are described in this section. The first subsection describes the inference of logical parameters from SMBioNet. The second subsection shows the results obtained by the qualitative modeling and analysis of the BRN using tool, GenoTech. The third subsection shows the network analysis of the BRN for extracting the most significant cycle. The outcomes obtained from hybrid modeling of the BRN are described in the fourth subsection.

4.1 Inference of logical parameters

The BRN given in (Figure 2.3) consist of four entities; namely AKT, NF-κB, HuR and GRB10 . Thresholds fixed by variables AKT, NF-κB, HuR and GRB10 lead to a total of 16 possible states in the state graph (Figure 4.1). The state vector (AKT, NF-κB, HuR, and GRB10) is used to represent the state of the system at any given time. Prior to the signaling of AKT, all the proteins that contribute in this network are absent. Hence, (AKT=1, NF-κB=0, HuR=0 and GRB10=0) represents the starting state of the system. According to the previous studies [11], the vicinity of two responses in the same system, infers the existence of two conceivable ways beginning from the

starting state i.e. (1000) that can proceed towards apoptosis and a cancerous state. [7, 36]. The normal state is known to be characterized by the low levels of all proteins, whereas the cancerous state is distinguished by the over-expression of AKT, NF-κB, HuR and GRB10. The loss of expression of any protein will not allow the activation of other protein which effects the positive feedback mechanism and hence results in an apoptotic state.

These perceptions are encoded in CTL equations as shown below.

$$Init = (AKT = 1 \quad \& \quad NF - \kappa B = 0 \quad \& \quad HuR = 0 \quad \& \quad GRB10 = 0) \tag{4.1}$$

$$Cancerous = (AKT = 1 \quad \& \quad NF - \kappa B = 1 \quad \& \quad HuR = 1 \quad \& \quad GRB10 = 1) \tag{4.2}$$

$$Apoptosis = (AKT = 0 \quad \& \quad NF - \kappa B = 0 \quad \& \quad HuR = 0 \quad \& \quad GRB10 = 0) \tag{4.3}$$

$$\phi_1 = Init \rightarrow AX(EF(Init)) \tag{4.4}$$

$$\phi_2 = Init \rightarrow EF(AG(Cancerous)) \tag{4.5}$$

$$\phi_3 = Init \rightarrow EF(AG(Apoptosis)) \tag{4.6}$$

$$\phi = \phi_1 \quad \& \quad \phi_2 \quad \& \quad \phi_3 \tag{4.7}$$

The first CTL property (Equation 4.4) represents that the system is quite able to maintain the homeostasis by returning to its initial position from where it started. The second property (Equation 4.5) models the conduct of the BRN that reflects that the cancerous state is reachable from an initial state and stays as its future state. If the future state endures for quite a while then we can call this as stable state. The third property (Equation 4.6) represents the state where loss of expression of all entities mediates the system towards apoptosis. The formula combines (conjuncts) these three properties (Equation 4.7) and generates sets of logical parameters via SMBioNet. SMBioNet selected 6 sets of parameters (each set represents a specific qualitative model) that satisfies the above mentioned CTL formula (See Supplementary File (A)). Among 6 models, the current model shown in table 4.1 was selected because it incorporates the above mentioned observations in the form of two stable states (cancerous/apoptotic) and homeostatic states. Additionally, we analyzed the selected model in GenoTech by generating the state graph as shown in Figure 4.1, which allowed us to analyze the expression pattern of the proteins, cyclic paths, stable states and the dynamics of the BRN.

Table 4.1: Table shows the selected set of parameters using SMBioNet tool

Parameter	Resource	Range of values	Selected values
K_{AKT}	{}	0	0
K_{AKT}	GRB10	0,1	1
$K_{NF-\kappa B}$	{}	0	0
$K_{NF-\kappa B}$	AKT	0,1	1
K_{HuR}	{}	0	0
K_{HuR}	NF-κB	0,1	1
K_{HuR}	{HuR, NF-κB}	0,1	1
K_{HuR}	HuR	0,1	0
K_{GRB10}	{}	0	0
K_{GRB10}	HuR	0,1	1

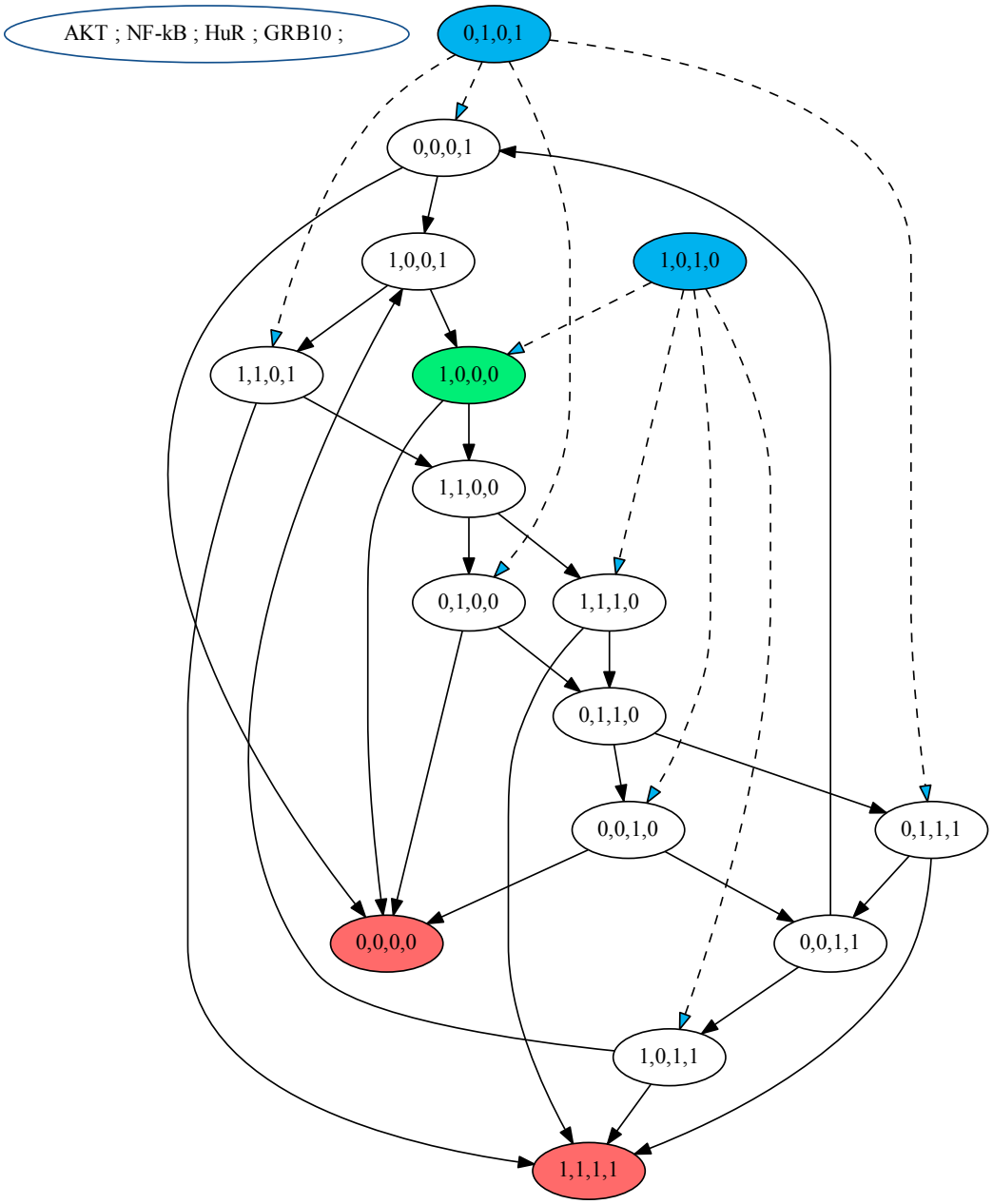

Figure 4.1: **Qualitative model of HuR associated pathway:** The graph shows the 16 possible states, based on the permutations of the discretised concentration levels of the constituent entities. State (1000), shown in green color, expresses the starting state of the system. States in blue color, (1010) and (0101), indicate the perturbed states which have no incoming transitions. The stable states are highlighted in red color where (1111) represents the over expression of all proteins which lead towards cancerous state, and (0000) shows the loss of expression of proteins that mediates apoptosis.

4.2 Qualitative modeling

The state graph represents all possible transitions from one state to another, where each state shows the expression level of every entity at a particular time. The qualitative model (Figure 4.1) of the HuR associated BRN encompasses three types of behaviors which include 16 cycles representing homeostasis, and two stable states (Cancerous and Apoptotic). Closed or cyclic paths represent the homeostasis of the system, nevertheless, a diseased state can be accomplished if homeostasis cannot be maintained. The 16 cycles (See Supplementary File (B)) obtained after generating state graph are time-abstract cycles, therefore, their exact nature cannot be predicted using qualitative modeling. Thus, discrete model was transformed in to hybrid model for further analysis. Diseased state can be experienced if cycles or closed paths in HuR pathway progress continuously towards the stable enduring state. From a stable state, which is like a sink, the system does not evolve to other states, so has been termed as stable state. The stable state (1111) as shown in red color represents the elevated level of all the entities, illustrating the cancerous behavior. The other stable state (0000) shows synergistic loss of expression of all the proteins. Additionally, the state graph contains two perturbed states, (0101) and (1010), which do not contain any incoming transitions. The eight bifurcation states (1101), (1000), (1110), (0100), (0111), (0010), and (1011) are states, which can lead the system either towards cyclic path or have stable state in their immediate successors. This demonstrated that the system will remain in the cycle (at normal physiological level), whereas the high level of all these proteins will divert the system to the stable (cancerous) state.

These insights highlighted the significance of all these proteins in normal and stressed conditions. Our findings conclude that the homeostasis can only be maintained if we could tightly regulate the expression level of proteins. The elevated level of all proteins will lead towards RCC, as evident from the state 1111, while synergistic loss of expression of these proteins will mediate the system towards apoptosis (0000).

4.3 Network analysis

The state graph was further analyzed using the network analysis techniques to select a cycle for hybrid modeling. The color spectrum from red to green in Figure 4.2 shows the betweenness centrality from low to high, respectively. It was observed that four states (0011), (1100), (1001), (0110) showed the highest betweenness centralities and were common in all cycles (represented in dark green color). From a biological perspective, states with higher betweenness centralities are the ones favored by the system due to their frequent occurrences [78]. Stable states (0000) and (1111) are characterized by zero betweenness centrality. With the added knowledge of centralities, the selection of a cycle for hybrid modeling initiated with the progressive selection of successors based on the centralities of the available successors at each state transition. Completely restricting to the highest betweenness centrality at every set of successors proved unfruitful since all cycles showed equal centralities due to the presence of high betweenness successors ((0011), (1100), (1001), (0110)) in every cycle. This adds a new dimension indicating that each cycle has equal probability for occurrence and is equally important in the network.

As previously mentioned, (See Introduction) AKT activation regulates HuR expression by transcriptional activation of HuR through $NF\kappa B$. Therefore, based on literature [11, 35] and HuR associated pathway ($AKT - NF\kappa B$) shown in (Figure 2.2), we proposed that (1000) constitutes the starting state of system as depicted in state graph (Figure 4.1). Thus, based on starting state (1000), finally eight cycles were extracted from 16 cycles to reduce the complexity of network (See Supplementary File (B)).

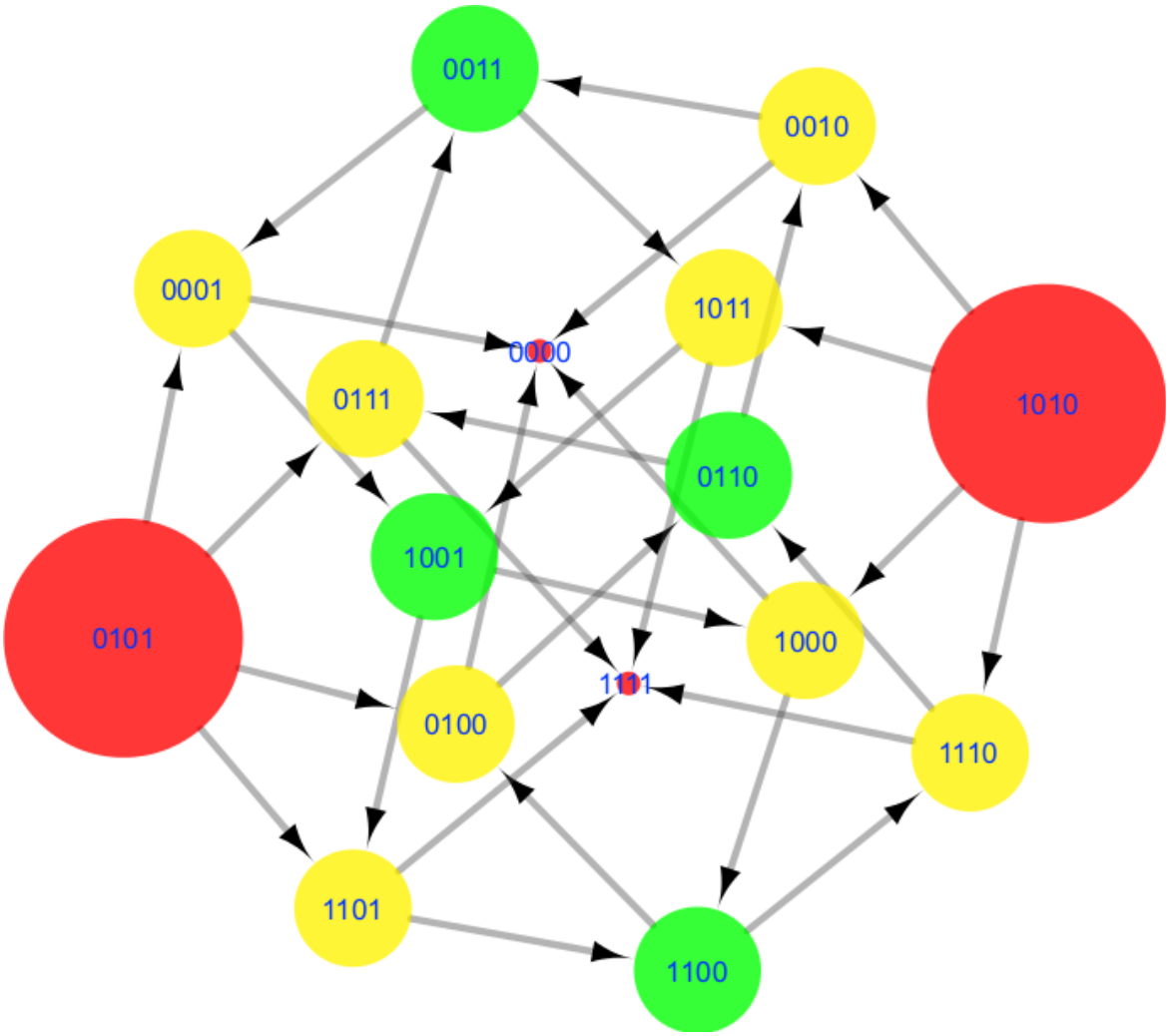

Figure 4.2: **Network analysis of state graph:** The state graph is visually representing the state centralities. The color spectrum from red to green indicates betweenness centrality from low to high respectively. Red color represents the least centrality, yellow shows average state cenrality and the green color depicts the highest betweenness centrality. Deadlocks are chracterized by zero betweenness centrality.

4.4 Hybrid modeling

In this subsection, we present the HyTech results regarding the convergence domain of the BRN. The discrete and continuous behaviors were incorporated in the qualitative model by refining with clock measuring regulation delays to produce a hybrid model. The delays endow us with the timing of activation and inhibition of the concerned proteins which control a particular set of trajectories ensuing in a cycle. If a conjuncted constraint relation of a convergence domain becomes false, the trajectories will diverge from cyclic path and might even enter in a stable (cancerous/apoptotic) state. The convergence domain computed for the selected cycles is shown in tables 4.2, 4.4, 4.6, 4.8, 4.10, 4.12, 4.14 and 4.16 respectively, detailing the delay constraints governing the trajectory. The tables additionally permits us to form a relation matrix ($\leq$, $<$, $\geq$, $>$, $=$) among the individual delays given in tables 4.3, 4.5, 4.7, 4.9, 4.11, 4.13, 4.15 and 4.17.

Table 4.2: Convergence domain of the 1^{st} cycle. The convergence domain shows the delay constraints that are satisfied in this cycle.

Convergence Domain	**Qualitative Cycle**	(0 0 0 1)→(1 0 0 1)→(1 0 0 0)→(1 1 0 0)→(0 1 0 0)→(0 1 1 0)→(0 0 1 0)→(0 0 1 1)→(0 0 0 1)
	Conjunction of constraints (I-XIII)	
	I	$d^+_{HUR} \geq \lvert d^-_{AKT}\rvert$
	II	$d^+_{AKT} \geq \lvert d^-_{HUR}\rvert$
	III	$d^+_{HUR} \leq \lvert d^-_{NF-\kappa B}\rvert + \lvert d^-_{AKT}\rvert$
	IV	$d^+_{NF-\kappa B} \leq \lvert d^-_{GRB10}\rvert + \lvert d^-_{AKT}\rvert$
	V	$d^+_{NF-\kappa B} + d^+_{GRB10} \leq d^+_{HUR} + \lvert d^-_{HUR}\rvert + \lvert d^-_{GRB10}\rvert$
	VI	$2d^+_{AKT} + d^+_{HUR} \leq d^+_{NF-\kappa B} + d^+_{GRB10} + \lvert d^-_{GRB10}\rvert + \lvert d^-_{HUR}\rvert$
	VII	$d^+_{AKT} + d^+_{HUR} \leq d^+_{GRB10} + \lvert d^-_{GRB10}\rvert + \lvert d^-_{AKT}\rvert$
	VIII	$d^+_{GRB10} \geq \lvert d^-_{NF-\kappa B}\rvert$
	IX	$d^+_{AKT} + d^+_{HUR} \leq d^+_{NF-\kappa B} + \lvert d^-_{NF-\kappa B}\rvert + \lvert d^-_{HUR}\rvert$
	X	$d^+_{GRB10} \leq \lvert d^-_{HUR}\rvert + \lvert d^-_{NF-\kappa B}\rvert$
	XI	$d^+_{NF-\kappa B} \leq d^+_{AKT} + \lvert d^-_{AKT}\rvert$
	XII	$d^+_{NF-\kappa B} + d^+_{GRB10} \leq d^+_{AKT} + d^+_{HUR} + \lvert d^-_{HUR}\rvert$
	XIII	$d^+_{NF-\kappa B} \geq \lvert d^-_{GRB10}\rvert$

Table 4.3: Relation Matrix of the 1^{st} cycle depicting binary relations between states.

Relational Matrix								
	d^+_{AKT}	$\lvert d^-_{AKT}\rvert$	$d^+_{NF-\kappa B}$	$\lvert d^-_{NF-\kappa B}\rvert$	d^+_{HUR}	$\lvert d^-_{HUR}\rvert$	d^+_{GRB10}	$\lvert d^-_{GRB10}\rvert$
d^+_{AKT}	$=$							
$\lvert d^-_{AKT}\rvert$	$\geq, \leq$	$=$						
$d^+_{NF-\kappa B}$	$\geq, \leq$	$\geq, \leq$	$=$					
$\lvert d^-_{NF-\kappa B}\rvert$	$\geq, \leq$	$\geq, \leq$	$\geq, \leq$	$=$				
d^+_{HUR}	$\geq, \leq$	$\geq$	$\geq, \leq$	$\geq, \leq$	$=$			
$\lvert d^-_{HUR}\rvert$	$\leq$	$\geq, \leq$	$\geq, \leq$	$\geq, \leq$	$\geq, \leq$	$=$		
d^+_{GRB10}	$\geq, \leq$	$\geq, \leq$	$\geq, \leq$	$\geq$	$\geq, \leq$	$\geq, \leq$	$=$	
$\lvert d^-_{GRB10}\rvert$	$\geq, \leq$	$\geq, \leq$	$\leq$	$\geq, \leq$	$\geq, \leq$	$\geq, \leq$	$\geq, \leq$	$=$

Table 4.4: Convergence domain of the 2^{nd} cycle. The convergence domain shows the delay constraints that are satisfied in this cycle.

Convergence Domain	**Qualitative Cycle**	(0 0 0 1)→(1 0 0 1)→(1 0 0 0)→(1 1 0 0)→(0 1 0 0)→(0 1 1 0)→(0 1 1 1)→(0 0 1 1)→(0 0 0 1)
	Conjunction of constraints (I-XV)	
	I	$d^+_{HUR} \geq \lvert d^-_{AKT}\rvert$
	II	$d^+_{GRB10} \leq \lvert d^-_{NF-\kappa B}\rvert$
	III	$d^+_{NF-\kappa B} + \lvert d^-_{NF-\kappa B}\rvert \leq d^+_{HUR} + \lvert d^-_{HUR}\rvert + \lvert d^-_{GRB10}\rvert$
	IV	$d^+_{NF-\kappa B} \leq \lvert d^-_{GRB10}\rvert + \lvert d^-_{AKT}\rvert$
	V	$d^+_{AKT} + d^+_{HUR} \leq d^+_{NF-\kappa B} + d^+_{GRB10} + \lvert d^-_{HUR}\rvert$
	VI	$2d^+_{AKT} + d^+_{HUR} \leq d^+_{NF-\kappa B} + \lvert d^-_{NF-\kappa B}\rvert + \lvert d^-_{GRB10}\rvert + \lvert d^-_{HUR}\rvert$
	VII	$d^+_{AKT} + d^+_{HUR} \leq d^+_{NF-\kappa B} + \lvert d^-_{NF-\kappa B}\rvert + d^+_{GRB10}$
	VIII	$2d^+_{AKT} + d^+_{HUR} \leq d^+_{NF-\kappa B} + 2\lvert d^-_{NF-\kappa B}\rvert + \lvert d^-_{GRB10}\rvert$
	IX	$d^+_{HUR} \leq d^+_{GRB10} + \lvert d^-_{AKT}\rvert$
	X	$d^+_{GRB10} + \lvert d^-_{HUR}\rvert \geq \lvert d^-_{NF-\kappa B}\rvert$
	XI	$d^+_{AKT} + d^+_{HUR} \leq \lvert d^-_{GRB10}\rvert + \lvert d^-_{NF-\kappa B}\rvert + \lvert d^-_{AKT}\rvert$
	XII	$d^+_{NF-\kappa B} + \lvert d^-_{NF-\kappa B}\rvert \leq d^+_{AKT} + d^+_{HUR} + \lvert d^-_{HUR}\rvert$
	XIII	$d^+_{NF-\kappa B} \leq d^+_{AKT} + \lvert d^-_{AKT}\rvert$
	XIV	$d^+_{AKT} \geq \lvert d^-_{HUR}\rvert$
	XV	$d^+_{NF-\kappa B} \geq \lvert d^-_{GRB10}\rvert$

Table 4.5: Relation Matrix of the 2^{nd} cycle depicting binary relations between states.

Relational Matrix								
	d^+_{AKT}	$\lvert d^-_{AKT}\rvert$	$d^+_{NF-\kappa B}$	$\lvert d^-_{NF-\kappa B}\rvert$	d^+_{HUR}	$\lvert d^-_{HUR}\rvert$	d^+_{GRB10}	$\lvert d^-_{GRB10}\rvert$
d^+_{AKT}	$=$							
$\lvert d^-_{AKT}\rvert$	$\geq, \leq$	$=$						
$d^+_{NF-\kappa B}$	$\geq, \leq$	$\geq, \leq$	$=$					
$\lvert d^-_{NF-\kappa B}\rvert$	$\geq, \leq$	$\geq, \leq$	$\geq, \leq$	$=$				
d^+_{HUR}	$\geq, \leq$	$\geq$	$\geq, \leq$	$\geq, \leq$	$=$			
$\lvert d^-_{HUR}\rvert$	$\leq$	$\geq, \leq$	$\geq, \leq$	$\geq, \leq$	$\geq, \leq$	$=$		
d^+_{GRB10}	$\geq, \leq$	$\geq, \leq$	$\geq, \leq$	$\leq$	$\geq, \leq$	$\geq, \leq$	$=$	
$\lvert d^-_{GRB10}\rvert$	$\geq, \leq$	$\geq, \leq$	$\leq$	$\geq, \leq$	$\geq, \leq$	$\geq, \leq$	$\geq, \leq$	$=$

Table 4.6: Convergence domain of the 3^{rd} cycle. The convergence domain shows the delay constraints that are satisfied in this cycle.

Convergence Domain	**Qualitative Cycle**	$(0\,0\,0\,1)\rightarrow(1\,0\,0\,1)\rightarrow(1\,0\,0\,0)\rightarrow(1\,1\,0\,0)\rightarrow(1\,1\,1\,0)\rightarrow(0\,1\,1\,0)\rightarrow(0\,0\,1\,0)\rightarrow(0\,0\,1\,1)\rightarrow(0\,0\,0\,1)$
	Conjunction of constraints (I-XIII)	
	I	$d^+_{HUR} \leq \lvert d^-_{AKT}\rvert$
	II	$d^+_{GRB10} \geq \lvert d^-_{NF-\kappa B}\rvert$
	III	$d^+_{HUR} + \lvert d^-_{NF-\kappa B}\rvert \geq \lvert d^-_{AKT}\rvert$
	IV	$d^+_{GRB10} \leq \lvert d^-_{HUR}\rvert + \lvert d^-_{NF-\kappa B}\rvert$
	V	$d^+_{NF-\kappa B} + d^+_{GRB10} \leq \lvert d^-_{GRB10}\rvert + \lvert d^-_{HUR}\rvert + \lvert d^-_{AKT}\rvert$
	VI	$d^+_{NF-\kappa B} \leq d^+_{HUR} + \lvert d^-_{GRB10}\rvert$
	VII	$d^+_{NF-\kappa B} \leq d^+_{AKT} + d^+_{HUR}$
	VIII	$d^+_{NF-\kappa B} + d^+_{GRB10} \leq d^+_{AKT} + \lvert d^-_{AKT}\rvert + \lvert d^-_{HUR}\rvert$
	IX	$d^+_{AKT} + \lvert d^-_{AKT}\rvert \leq d^+_{GRB10} + \lvert d^-_{GRB10}\rvert + d^+_{HUR}$
	X	$d^+_{AKT} + \lvert d^-_{AKT}\rvert \leq d^+_{NF-\kappa B} + \lvert d^-_{NF-\kappa B}\rvert + \lvert d^-_{HUR}\rvert$
	XI	$2d^+_{AKT} + \lvert d^-_{AKT}\rvert \leq d^+_{NF-\kappa B} + d^+_{GRB10} + \lvert d^-_{GRB10}\rvert + \lvert d^-_{HUR}\rvert$
	XII	$d^+_{AKT} \geq \lvert d^-_{HUR}\rvert$
	XIII	$d^+_{NF-\kappa B} \geq \lvert d^-_{GRB10}\rvert$

Table 4.7: Relation Matrix of the 3^{rd} cycle depicting binary relations between states.

Relational Matrix								
	d^+_{AKT}	$\lvert d^-_{AKT}\rvert$	$d^+_{NF-\kappa B}$	$\lvert d^-_{NF-\kappa B}\rvert$	d^+_{HUR}	$\lvert d^-_{HUR}\rvert$	d^+_{GRB10}	$\lvert d^-_{GRB10}\rvert$
d^+_{AKT}	$=$							
$\lvert d^-_{AKT}\rvert$	$\geq, \leq$	$=$						
$d^+_{NF-\kappa B}$	$\geq, \leq$	$\geq, \leq$	$=$					
$\lvert d^-_{NF-\kappa B}\rvert$	$\geq, \leq$	$\geq, \leq$	$\geq, \leq$	$=$				
d^+_{HUR}	$\geq, \leq$	$\geq$	$\geq, \leq$	$\geq, \leq$	$=$			
$\lvert d^-_{HUR}\rvert$	$\leq$	$\geq, \leq$	$\geq, \leq$	$\geq, \leq$	$\geq, \leq$	$=$		
d^+_{GRB10}	$\geq, \leq$	$\geq, \leq$	$\geq, \leq$	$\geq$	$\geq, \leq$	$\geq, \leq$	$=$	
$\lvert d^-_{GRB10}\rvert$	$\geq, \leq$	$\geq, \leq$	$\leq$	$\geq, \leq$	$\geq, \leq$	$\geq, \leq$	$\geq, \leq$	$=$

Table 4.8: Convergence domain of the 4^{th} cycle. The convergence domain shows the delay constraints that are satisfied in this cycle.

Convergence Domain	**Qualitative Cycle**	$(0\,0\,0\,1)\rightarrow(1\,0\,0\,1)\rightarrow(1\,0\,0\,0)\rightarrow(1\,1\,0\,0)\rightarrow(1\,1\,1\,0)\rightarrow(0\,1\,1\,0)\rightarrow(0\,1\,1\,1)\rightarrow(0\,0\,1\,1)\rightarrow(0\,0\,0\,1)$
	Conjunction of constraints (I-XV)	
	I	$d^+_{HUR} \leq \lvert d^-_{AKT}\rvert$
	II	$d^+_{GRB10} \leq \lvert d^-_{NF-\kappa B}\rvert$
	III	$d^+_{NF-\kappa B} + \lvert d^-_{NF-\kappa B}\rvert \leq \lvert d^-_{GRB10}\rvert + \lvert d^-_{HUR}\rvert + \lvert d^-_{AKT}\rvert$
	IV	$d^+_{NF-\kappa B} \leq d^+_{HUR} + \lvert d^-_{GRB10}\rvert$
	V	$d^+_{AKT} + \lvert d^-_{AKT}\rvert \leq d^+_{NF-\kappa B} + d^+_{GRB10} + \lvert d^-_{HUR}\rvert$
	VI	$2d^+_{AKT} + \lvert d^-_{AKT}\rvert \leq d^+_{NF-\kappa B} + \lvert d^-_{GRB10}\rvert + \lvert d^-_{HUR}\rvert + \lvert d^-_{NF-\kappa B}\rvert$
	VII	$d^+_{AKT} + \lvert d^-_{AKT}\rvert \leq d^+_{NF-\kappa B} + d^+_{GRB10} + \lvert d^-_{NF-\kappa B}\rvert$
	VIII	$2d^+_{AKT} + \lvert d^-_{AKT}\rvert \leq d^+_{NF-\kappa B} + \lvert d^-_{GRB10}\rvert + 2\lvert d^-_{NF-\kappa B}\rvert$
	IX	$d^+_{GRB10} + d^+_{HUR} \geq \lvert d^-_{AKT}\rvert$
	X	$\lvert d^-_{NF-\kappa B}\rvert \leq d^+_{GRB10} + \lvert d^-_{HUR}\rvert$
	XI	$d^+_{AKT} + \lvert d^-_{AKT}\rvert \leq d^+_{HUR} + \lvert d^-_{GRB10}\rvert + \lvert d^-_{NF-\kappa B}\rvert$
	XII	$d^+_{NF-\kappa B} + \lvert d^-_{NF-\kappa B}\rvert \leq d^+_{AKT} + \lvert d^-_{HUR}\rvert + \lvert d^-_{AKT}\rvert$
	XIII	$d^+_{NF-\kappa B} \leq d^+_{AKT} + d^+_{HUR}$
	XIV	$d^+_{AKT} \geq \lvert d^-_{HUR}\rvert$
	XV	$d^+_{NF-\kappa B} \geq \lvert d^-_{GRB10}\rvert$

Table 4.9: Relation Matrix of the 4^{th} cycle depicting binary relations between states.

Relational Matrix								
	d^+_{AKT}	$\lvert d^-_{AKT}\rvert$	$d^+_{NF-\kappa B}$	$\lvert d^-_{NF-\kappa B}\rvert$	d^+_{HUR}	$\lvert d^-_{HUR}\rvert$	d^+_{GRB10}	$\lvert d^-_{GRB10}\rvert$
d^+_{AKT}	$=$							
$\lvert d^-_{AKT}\rvert$	$\geq, \leq$	$=$						
$d^+_{NF-\kappa B}$	$\geq, \leq$	$\geq, \leq$	$=$					
$\lvert d^-_{NF-\kappa B}\rvert$	$\geq, \leq$	$\geq, \leq$	$\geq, \leq$	$=$				
d^+_{HUR}	$\geq, \leq$	$\leq$	$\geq, \leq$	$\geq, \leq$	$=$			
$\lvert d^-_{HUR}\rvert$	$\leq$	$\geq, \leq$	$\geq, \leq$	$\geq, \leq$	$\geq, \leq$	$=$		
d^+_{GRB10}	$\geq, \leq$	$\geq, \leq$	$\geq, \leq$	$\leq$	$\geq, \leq$	$\geq, \leq$	$=$	
$\lvert d^-_{GRB10}\rvert$	$\geq, \leq$	$\geq, \leq$	$\leq$	$\geq, \leq$	$\geq, \leq$	$\geq, \leq$	$\geq, \leq$	$=$

Table 4.10: Convergence domain of the 5^{th} cycle. The convergence domain shows the delay constraints that are satisfied in this cycle.

Convergence Domain	**Qualitative Cycle**	(0 0 1 0)→(0 0 1 1)→(1 0 1 1)→(1 0 0 1)→(1 0 0 0)→(1 1 0 0)→(0 1 0 0)→(0 1 1 0)→(0 0 1 0)
	Conjunction of constraints (I-XIII)	
	I	$d^+_{HUR} \geq \lvert d^-_{AKT}\rvert$
	II	$d^+_{GRB10} \geq \lvert d^-_{NF-\kappa B}\rvert$
	III	$d^+_{HUR} \leq \lvert d^-_{NF-\kappa B}\rvert + \lvert d^-_{AKT}\rvert$
	IV	$d^+_{GRB10} \leq d^+_{AKT} + \lvert d^-_{NF-\kappa B}\rvert$
	V	$d^+_{NF-\kappa B} + d^+_{GRB10} \leq d^+_{AKT} + d^+_{HUR} + \lvert d^-_{GRB10}\rvert$
	VI	$d^+_{NF-\kappa B} \leq \lvert d^-_{GRB10}\rvert + \lvert d^-_{AKT}\rvert$
	VII	$d^+_{NF-\kappa B} \leq \lvert d^-_{HUR}\rvert + \lvert d^-_{AKT}\rvert$
	VIII	$d^+_{NF-\kappa B} + d^+_{GRB10} \leq d^+_{AKT} + d^+_{HUR} + \lvert d^-_{HUR}\rvert$
	IX	$d^+_{HUR} + \lvert d^-_{HUR}\rvert \leq d^+_{GRB10} + \lvert d^-_{GRB10}\rvert + \lvert d^-_{AKT}\rvert$
	X	$d^+_{HUR} + \lvert d^-_{HUR}\rvert \leq d^+_{AKT} + d^+_{NF-\kappa B} + \lvert d^-_{NF-\kappa B}\rvert$
	XI	$d^+_{HUR} + 2\lvert d^-_{HUR}\rvert \leq d^+_{AKT} + d^+_{NF-\kappa B} + d^+_{GRB10} + \lvert d^-_{GRB10}\rvert$
	XII	$d^+_{AKT} \leq \lvert d^-_{HUR}\rvert$
	XIII	$d^+_{NF-\kappa B} \geq \lvert d^-_{GRB10}\rvert$

Table 4.11: Relation Matrix of the 5^{th} cycle depicting binary relations between states.

Relational Matrix								
	d^+_{AKT}	$\lvert d^-_{AKT}\rvert$	$d^+_{NF-\kappa B}$	$\lvert d^-_{NF-\kappa B}\rvert$	d^+_{HUR}	$\lvert d^-_{HUR}\rvert$	d^+_{GRB10}	$\lvert d^-_{GRB10}\rvert$
d^+_{AKT}	$=$							
$\lvert d^-_{AKT}\rvert$	$\geq, \leq$	$=$						
$d^+_{NF-\kappa B}$	$\geq, \leq$	$\geq, \leq$	$=$					
$\lvert d^-_{NF-\kappa B}\rvert$	$\geq, \leq$	$\geq, \leq$	$\geq, \leq$	$=$				
d^+_{HUR}	$\geq, \leq$	$\geq$	$\geq, \leq$	$\geq, \leq$	$=$			
$\lvert d^-_{HUR}\rvert$	$\geq$	$\geq, \leq$	$\geq, \leq$	$\geq, \leq$	$\geq, \leq$	$=$		
d^+_{GRB10}	$\geq, \leq$	$\geq, \leq$	$\geq, \leq$	$\geq$	$\geq, \leq$	$\geq, \leq$	$=$	
$\lvert d^-_{GRB10}\rvert$	$\geq, \leq$	$\geq, \leq$	$\leq$	$\geq, \leq$	$\geq, \leq$	$\geq, \leq$	$\geq, \leq$	$=$

Table 4.12: Convergence domain of the 6^{th} cycle. The convergence domain shows the delay constraints that are satisfied in this cycle.

Convergence Domain	**Qualitative Cycle**	(0 0 1 0)→(0 0 1 1)→(1 0 1 1)→(1 0 0 1)→(1 0 0 0)→(1 1 0 0)→(1 1 1 0)→(0 1 1 0)→(0 0 1 0)
	Conjunction of constraints (I-XIII)	
	I	$d^+_{HUR} \leq \lvert d^-_{AKT}\rvert$
	II	$d^+_{GRB10} \geq \lvert d^-_{NF-\kappa B}\rvert$
	III	$d^+_{HUR} + \lvert d^-_{NF-\kappa B}\rvert \geq \lvert d^-_{AKT}\rvert$
	IV	$d^+_{GRB10} \leq d^+_{AKT} + \lvert d^-_{NF-\kappa B}\rvert$
	V	$d^+_{NF-\kappa B} + d^+_{GRB10} \leq d^+_{AKT} + \lvert d^-_{AKT}\rvert + \lvert d^-_{GRB10}\rvert$
	VI	$d^+_{NF-\kappa B} \leq d^+_{HUR} + \lvert d^-_{GRB10}\rvert$
	VII	$d^+_{NF-\kappa B} \leq d^+_{HUR} + \lvert d^-_{HUR}\rvert$
	VIII	$d^+_{NF-\kappa B} + d^+_{GRB10} \leq d^+_{AKT} + \lvert d^-_{AKT}\rvert + \lvert d^-_{HUR}\rvert$
	IX	$\lvert d^-_{HUR}\rvert + \lvert d^-_{AKT}\rvert \leq d^+_{GRB10} + \lvert d^-_{GRB10}\rvert + d^+_{HUR}$
	X	$\lvert d^-_{HUR}\rvert + \lvert d^-_{AKT}\rvert \leq d^+_{AKT} + d^+_{NF-\kappa B} + \lvert d^-_{NF-\kappa B}\rvert$
	XI	$2\lvert d^-_{HUR}\rvert + \lvert d^-_{AKT}\rvert \leq d^+_{AKT} + d^+_{NF-\kappa B} + d^+_{GRB10} + \lvert d^-_{GRB10}\rvert$
	XII	$d^+_{AKT} \leq \lvert d^-_{HUR}\rvert$
	XIII	$d^+_{NF-\kappa B} \geq \lvert d^-_{GRB10}\rvert$

Table 4.13: Relation Matrix of the 6^{th} cycle depicting binary relations between states.

Relational Matrix								
	d^+_{AKT}	$\lvert d^-_{AKT}\rvert$	$d^+_{NF-\kappa B}$	$\lvert d^-_{NF-\kappa B}\rvert$	d^+_{HUR}	$\lvert d^-_{HUR}\rvert$	d^+_{GRB10}	$\lvert d^-_{GRB10}\rvert$
d^+_{AKT}	$=$							
$\lvert d^-_{AKT}\rvert$	$\geq, \leq$	$=$						
$d^+_{NF-\kappa B}$	$\geq, \leq$	$\geq, \leq$	$=$					
$\lvert d^-_{NF-\kappa B}\rvert$	$\geq, \leq$	$\geq, \leq$	$\geq, \leq$	$=$				
d^+_{HUR}	$\geq, \leq$	$\leq$	$\geq, \leq$	$\geq, \leq$	$=$			
$\lvert d^-_{HUR}\rvert$	$\geq$	$\geq, \leq$	$\geq, \leq$	$\geq, \leq$	$\geq, \leq$	$=$		
d^+_{GRB10}	$\geq, \leq$	$\geq, \leq$	$\geq, \leq$	$\geq$	$\geq, \leq$	$\geq, \leq$	$=$	
$\lvert d^-_{GRB10}\rvert$	$\geq, \leq$	$\geq, \leq$	$\leq$	$\geq, \leq$	$\geq, \leq$	$\geq, \leq$	$\geq, \leq$	$=$

Table 4.14: Convergence domain of the 7^{th} cycle. The convergence domain shows the delay constraints that are satisfied in this cycle.

Convergence Domain	**Qualitative Cycle**	(0 0 1 1)→(1 0 1 1)→(1 0 0 1)→(1 0 0 0)→(1 1 0 0)→(0 1 0 0)→(0 1 1 0)→(0 1 1 1)→(0 0 1 1)
	Conjunction of constraints (I-XV)	
	I	$d^+_{HUR} \geq \lvert d^-_{AKT}\rvert$
	II	$d^+_{HUR} \leq d^+_{GRB10} + \lvert d^-_{AKT}\rvert$
	III	$d^+_{NF-\kappa B} \leq \lvert d^-_{GRB10}\rvert + \lvert d^-_{AKT}\rvert$
	IV	$d^+_{NF-\kappa B} + \lvert d^-_{NF-\kappa B}\rvert \leq d^+_{AKT} + d^+_{HUR} + \lvert d^-_{GRB10}\rvert$
	V	$d^+_{HUR} + \lvert d^-_{HUR}\rvert \leq d^+_{AKT} + d^+_{NF-\kappa B} + d^+_{GRB10}$
	VI	$d^+_{HUR} + \lvert d^-_{HUR}\rvert \leq d^+_{NF-\kappa B} + \lvert d^-_{NF-\kappa B}\rvert + d^+_{GRB10}$
	VII	$d^+_{HUR} + 2\lvert d^-_{HUR}\rvert \leq d^+_{NF-\kappa B} + 2\lvert d^-_{NF-\kappa B}\rvert + \lvert d^-_{GRB10}\rvert$
	VIII	$d^+_{HUR} + \lvert d^-_{HUR}\rvert \leq \lvert d^-_{GRB10}\rvert + \lvert d^-_{NF-\kappa B}\rvert + \lvert d^-_{AKT}\rvert$
	IX	$d^+_{HUR} + 2\lvert d^-_{HUR}\rvert \leq d^+_{AKT} + \lvert d^-_{GRB10}\rvert + d^+_{NF-\kappa B} + \lvert d^-_{NF-\kappa B}\rvert$
	X	$d^+_{GRB10} \leq \lvert d^-_{NF-\kappa B}\rvert$
	XI	$d^+_{NF-\kappa B} \leq + \lvert d^-_{HUR}\rvert + \lvert d^-_{AKT}\rvert$
	XII	$d^+_{NF-\kappa B} + \lvert d^-_{NF-\kappa B}\rvert \leq d^+_{AKT} + d^+_{HUR} + \lvert d^-_{HUR}\rvert$
	XIII	$d^+_{AKT} + d^+_{GRB10} \geq \lvert d^-_{NF-\kappa B}\rvert$
	XIV	$d^+_{AKT} \leq \lvert d^-_{HUR}\rvert$
	XV	$d^+_{NF-\kappa B} \geq \lvert d^-_{GRB10}\rvert$

Table 4.15: Relation Matrix of the 7^{th} cycle depicting binary relations between states.

Relational Matrix								
	d^+_{AKT}	$\lvert d^-_{AKT}\rvert$	$d^+_{NF-\kappa B}$	$\lvert d^-_{NF-\kappa B}\rvert$	d^+_{HUR}	$\lvert d^-_{HUR}\rvert$	d^+_{GRB10}	$\lvert d^-_{GRB10}\rvert$
d^+_{AKT}	$=$							
$\lvert d^-_{AKT}\rvert$	$\geq, \leq$	$=$						
$d^+_{NF-\kappa B}$	$\geq, \leq$	$\geq, \leq$	$=$					
$\lvert d^-_{NF-\kappa B}\rvert$	$\geq, \leq$	$\geq, \leq$	$\geq, \leq$	$=$				
d^+_{HUR}	$\geq, \leq$	$\geq$	$\geq, \leq$	$\geq, \leq$	$=$			
$\lvert d^-_{HUR}\rvert$	$\geq$	$\geq, \leq$	$\geq, \leq$	$\geq, \leq$	$\geq, \leq$	$=$		
d^+_{GRB10}	$\geq, \leq$	$\geq, \leq$	$\geq, \leq$	$\leq$	$\geq, \leq$	$\geq, \leq$	$=$	
$\lvert d^-_{GRB10}\rvert$	$\geq, \leq$	$\geq, \leq$	$\leq$	$\geq, \leq$	$\geq, \leq$	$\geq, \leq$	$\geq, \leq$	$=$

Table 4.16: Convergence domain of the 8^{th} cycle. The convergence domain shows the delay constraints that are satisfied in this cycle.

Convergence Domain	**Qualitative Cycle**	(0 0 1 1)→(1 0 1 1)→(1 0 0 1)→(1 0 0 0)→(1 1 0 0)→(1 1 1 0)→(0 1 1 0)→(0 1 1 1)→(0 0 1 1)
	Conjunction of constraints (I-XV)	
	I	$d^+_{HUR} \leq \lvert d^-_{AKT}\rvert$
	II	$d^+_{GRB10} + d^+_{HUR} \geq \lvert d^-_{AKT}\rvert$
	III	$d^+_{NF-\kappa B} \leq d^+_{HUR} + \lvert d^-_{GRB10}\rvert$
	IV	$d^+_{NF-\kappa B} + \lvert d^-_{NF-\kappa B}\rvert \leq d^+_{AKT} + \lvert d^-_{AKT}\rvert + \lvert d^-_{GRB10}\rvert$
	V	$d^+_{AKT} + d^+_{NF-\kappa B} + d^+_{GRB10} \geq \lvert d^-_{HUR}\rvert + \lvert d^-_{AKT}\rvert$
	VI	$\lvert d^-_{HUR}\rvert + \lvert d^-_{AKT}\rvert \leq d^+_{NF-\kappa B} + \lvert d^-_{NF-\kappa B}\rvert + d^+_{GRB10}$
	VII	$2\lvert d^-_{HUR}\rvert + \lvert d^-_{AKT}\rvert \leq d^+_{NF-\kappa B} + 2\lvert d^-_{NF-\kappa B}\rvert + \lvert d^-_{GRB10}\rvert$
	VIII	$\lvert d^-_{AKT}\rvert + \lvert d^-_{HUR}\rvert + \leq d^+_{HUR} + \lvert d^-_{NF-\kappa B}\rvert + \lvert d^-_{GRB10}\rvert$
	IX	$2\lvert d^-_{HUR}\rvert + \lvert d^-_{AKT}\rvert \leq d^+_{AKT} + d^+_{NF-\kappa B} + \lvert d^-_{NF-\kappa B}\rvert + \lvert d^-_{GRB10}\rvert$
	X	$d^+_{GRB10} \leq \lvert d^-_{NF-\kappa B}\rvert$
	XI	$d^+_{NF-\kappa B} \leq d^+_{HUR} + \lvert d^-_{HUR}\rvert$
	XII	$d^+_{NF-\kappa B} + \lvert d^-_{NF-\kappa B}\rvert \leq d^+_{AKT} + \lvert d^-_{AKT}\rvert + \lvert d^-_{HUR}\rvert$
	XIII	$d^+_{AKT} + d^+_{GRB10} \geq \lvert d^-_{NF-\kappa B}\rvert$
	XIV	$d^+_{AKT} \leq \lvert d^-_{HUR}\rvert$
	XV	$d^+_{NF-\kappa B} \geq \lvert d^-_{GRB10}\rvert$

Table 4.17: Relation Matrix of the 8^{th} cycle depicting binary relations between states.

Relational Matrix								
	d^+_{AKT}	$\lvert d^-_{AKT}\rvert$	$d^+_{NF-\kappa B}$	$\lvert d^-_{NF-\kappa B}\rvert$	d^+_{HUR}	$\lvert d^-_{HUR}\rvert$	d^+_{GRB10}	$\lvert d^-_{GRB10}\rvert$
d^+_{AKT}	$=$							
$\lvert d^-_{AKT}\rvert$	$\geq, \leq$	$=$						
$d^+_{NF-\kappa B}$	$\geq, \leq$	$\geq, \leq$	$=$					
$\lvert d^-_{NF-\kappa B}\rvert$	$\geq, \leq$	$\geq, \leq$	$\geq, \leq$	$=$				
d^+_{HUR}	$\geq, \leq$	$\leq$	$\geq, \leq$	$\geq, \leq$	$=$			
$\lvert d^-_{HUR}\rvert$	$\geq$	$\geq, \leq$	$\geq, \leq$	$\geq, \leq$	$\geq, \leq$	$=$		
d^+_{GRB10}	$\geq, \leq$	$\geq, \leq$	$\geq, \leq$	$\leq$	$\geq, \leq$	$\geq, \leq$	$=$	
$\lvert d^-_{GRB10}\rvert$	$\geq, \leq$	$\geq, \leq$	$\leq$	$\geq, \leq$	$\geq, \leq$	$\geq, \leq$	$\geq, \leq$	$=$

The most significant delay constraint which is common in every cycle is $d^{+}_{NF\kappa B} \geq |d^{-}_{GRB10}|$. The two promising targets came in the result of hybrid modeling are the transcription factor NF-κB and adaptor protein GRb10. NF-κB is very important and unique in a way that it regulates all the important aspects of RCC, by aiding in HuR transcription. Constitutive activation of NF-κB in positive feedback loop can up regulate the level of many cyclins which are involved in uncontrolled proliferation [87]. The constraint shown above is common in all the cyclic trajectories. It explains that in order to maintain the homeostasis, degradation rate of GRB10 must be higher than the activation rate of NF-κB. However, the violation of this constraint will diverge the system in one of the stable (unfavorable) states. So, these factors appear to be an attractive target of new drugs for RCC. Oka et al. have recently revealed that inhibition of NF-κB phosphorylation by sesquiterpene lactone parthenolide in mice slows down RCC tumor growth through induction of tumor cell apoptosis [63]. Oya et al. investigated the 45 cases of human RCC, out of which 15 cases confirms a boost of greater than 200% in NF-κB activity compared with equivalent normal renal tissue [62]. Similarly, several comprehensive studies on the biological activity of HuR shows that it is a an important regulator of post-transcriptional gene expression and plays a vital role in cancer, thus its necessary to limit the rapid production of cytokines which aid in HuR transcription. Its various functions are associated with its ability to identify, bind, and stabilize a large subset of ARE-containing mRNAs. Previous studies reported that NF-κB and HuR maybe targeted against RCC. Since complete knock down of NF-κB would, on the other hand, prove harmful as it is essential for maintaining homeostasis of the immune system and is involved in many important cellular activities. HuR osciallation is equally vital against the RCC. Hence, we suggest that GRB10 maybe a better target as compared to NF-κB and HuR. Singh et.al. investigated that suppression of Grb10 can result in the loss of HuR mRNA, and suggested that Akt and NF-κB signaling are likely to regulate HuR transcription [11]. Our results also verify their study and suggests that suppression of GRB10 would

be advantageous. Therefore, while designing drugs against RCC, the expression level of GRB10 must be down regulated by using siRNAś or by designing such inhibitors for GRB10 which keep them suppressed. This would eventually lower the activation rate of NF-κB and helps in loss of HuR expression. The current study helps us to understand the molecular mechanism of HuR regulation and helped us to identify new target for drug design. The above findings urge that suppression of GRB10 can result in the maintenance of homeostasis by lowering the production rate of NF-κB, which regulates HuR transcription. The present study therefore, confirms that targeting GRB10 in HuR associated pathway can act as therapeutic and prognostic marker against RCC.

Part IV

Concluding the study

Chapter 5

Conclusion

In this thesis, the qualitative and hybrid models were constructed to predict the important insights into the dynamics of the HuR associated pathway. The qualitative model predicted steady state behaviors in the form of fifteen cycles and the two stable states. The cycles represented the homeostatic behavior of all the proteins. The stable state (1111) showed the elevated level of the proteins which lead towards cancerous state. The other stable state (0000) represented the down regulation of the proteins which can mediate apoptosis. The parameters of the qualitative model were predicted by using model-checking approach implemented in SMBioNet. The refined model with clock variables and delay parameters also called BIO-LHA of the HuR pathway was analyzed in HyTech to predict delays of the so-called convergence domains. The delays were characterized by linear parametric constraints. The relation matrices were computed and important constraints were analyzed to predict important protein for the treatment of RCC. These analysis suggest that GRB10 can be a drug target since the degradation delay of GRB10 was less than the activation delay of NF-κB. This constraint was observed in all the convergence domains. This study therefore, suggests that GRB10 maybe a potential drug target. In the light of these predictions, future studies can be carried out to validate this prediction.

Part V

Appendices and Bibliography

Bibliography

[1] American Cancer Society. Global health. http://www.cancer.org/aboutus/globalhealth/, 2014.

[2] E Comperat and P Camparo. Histological classification of malignant renal tumours at a time of major diagnostic and therapeutic changes. *Diagnostic and interventional imaging*, 93(4):221–231, 2012.

[3] American Cancer Society. Kidney cancer (adult) - renal cell carcinoma. http://www.cancer.org/acs/groups/cid/documents/webcontent/003107-pdf.pdf, 2014.

[4] VHL von Hippel-Lindau. Genetics of kidney cancer (renal cell cancer)(pdq®).

[5] Petros Sountoulides, Linda Metaxa, and Luca Cindolo. Atypical presentations and rare metastatic sites of renal cell carcinoma: a review of case reports. *J Med Case Rep*, 5(7):429, 2011.

[6] Wengong Wang, M Craig Caldwell, Shankung Lin, Henry Furneaux, and Myriam Gorospe. Hur regulates cyclin a and cyclin b1 mrna stability during cell proliferation. *The EMBO journal*, 19(10):2340–2350, 2000.

[7] Jun Wang, Yan Guo, Huili Chu, Yaping Guan, Jingwang Bi, and Baocheng Wang. Multiple functions of the rna-binding protein hur in cancer progression, treatment responses and prognosis. *International journal of molecular sciences*, 14(5):10015–10041, 2013.

[8] Hanna Ronkainen, Markku H Vaarala, Pasi Hirvikoski, and Ari Ristimäki. Hur expression is a marker of poor prognosis in renal cell carcinoma. *Tumor Biology*, 32(3):481–487, 2011.

[9] Sabrina Danilin, Carole Sourbier, Lionel Thomas, Sylvie Rothhut, Véronique Lindner, Jean-Jacques Helwig, Didier Jacqmin, Hervé Lang, and Thierry Massfelder. von hippel-lindau tumor suppressor gene-dependent mrna stabilization of the survival factor parathyroid hormone-related protein in human renal cell carcinoma by the rna-binding protein hur. *Carcinogenesis*, 30(3):387–396, 2009.

[10] Thierry Massfelder, Herve Lang, Eric Schordan, Veronique Lindner, Sylvie Rothhut, Sandra Welsch, Patricia Simon-Assmann, Mariette Barthelmebs, Didier Jacqmin, and Jean-Jacques Helwig. Parathyroid hormone-related protein is an essential growth factor for human clear cell renal carcinoma and a target for the von hippel-lindau tumor suppressor gene. *Cancer research*, 64(1):180–188, 2004.

[11] Mamata Singh, Alaina R Martinez, Suman Govindaraju, and Beth S Lee. Hur inhibits apoptosis by amplifying akt signaling through a positive feedback loop. *Journal of cellular physiology*, 228(1):182–189, 2013.

[12] Thomas Jahn, Petra Seipel, Susanne Urschel, Christian Peschel, and Justus Duyster. Role for the adaptor protein grb10 in the activation of akt. *Molecular and cellular biology*, 22(4):979–991, 2002.

[13] Nicolette K Janzen, Hyung L Kim, Robert A Figlin, and Arie S Belldegrun. Surveillance after radical or partial nephrectomy for localized renal cell carcinoma and management of recurrent disease. *Urologic Clinics of North America*, 30(4):843–852, 2003.

[14] PH Patel, RSK Chaganti, and RJ Motzer. Targeted therapy for metastatic renal cell carcinoma. *British journal of cancer*, 94(5):614–619, 2006.

[15] Nikolaos Grivas, Vasilios Kafarakis, Ioannis Tsimaris, Pavlos Raptis, Konstantinos Hastazeris, and Nikolaos E Stavropoulos. Clinico-pathological prognostic factors of renal cell carcinoma: A 15-year review from a single center in greece. *Urology annals*, 6(2):116, 2014.

[16] Chaan S Ng, Christopher G Wood, Paul M Silverman, Nizar M Tannir, Pheroze Tamboli, and Carl M Sandler. Renal cell carcinoma: diagnosis, staging, and surveillance. *American journal of roentgenology*, 191(4):1220–1232, 2008.

[17] W Linehan, Mcclellan M Walther, and Berton Zbar. The genetic basis of cancer of the kidney. *The Journal of urology*, 170(6):2163–2172, 2003.

[18] Antonio Lopez-Beltran, Marina Scarpelli, Rodolfo Montironi, and Ziya Kirkali. 2004 who classification of the renal tumors of the adults. *European urology*, 49(5):798–805, 2006.

[19] Borje Ljungberg, Karim Bensalah, Steven Canfield, Saeed Dabestani, Fabian Hofmann, Milan Hora, Markus A Kuczyk, Thomas Lam, Lorenzo Marconi, Axel S Merseburger, et al. Eau guidelines on renal cell carcinoma: 2014 update. *European urology*, 2015.

[20] G Mickisch, J Carballido, S Hellsten, H Schulze, and H Mensink. Guidelines on renal cell cancer. *UPDATE*, 2002.

[21] Wong-Ho Chow, Linda M Dong, and Susan S Devesa. Epidemiology and risk factors for kidney cancer. *Nature Reviews Urology*, 7(5):245–257, 2010.

[22] Bernard Escudier, Tim Eisen, Walter M Stadler, Cezary Szczylik, Stéphane Oudard, Michael Siebels, Sylvie Negrier, Christine Chevreau, Ewa Solska, Apurva A Desai, et al. Sorafenib in advanced clear-cell renal-cell carcinoma. *New England Journal of Medicine*, 356(2):125–134, 2007.

[23] David J Grignon and Mingxin Che. Clear cell renal cell carcinoma. *Clinics in laboratory medicine*, 25(2):305–316, 2005.

[24] Linda A Murakata, Kamal G Ishak, and Ugochukwu C Nzeako. Clear cell carcinoma of the liver: a comparative immunohistochemical study with renal clear cell carcinoma. *Modern Pathology*, 13(8):874–881, 2000.

[25] Robert J Motzer, Brian I Rini, Ronald M Bukowski, Brendan D Curti, Daniel J George, Gary R Hudes, Bruce G Redman, Kim A Margolin, Jaime R Merchan, George Wilding, et al. Sunitinib in patients with metastatic renal cell carcinoma. *Jama*, 295(21):2516–2524, 2006.

[26] E van den Berg and S Storkel. Kidney: renal cell carcinoma. atlas genet cytogenet oncol haematol. 2003.

[27] Michaël Peyromaure, Vincent Misrai, Nicolas Thiounn, Annick Vieillefond, Marc Zerbib, Thierry A Flam, and Bernard Debré. Chromophobe renal cell carcinoma. *Cancer*, 100(7):1406–1410, 2004.

[28] John N Eble. *Pathology and genetics of tumours of the urinary system and male genital organs*, volume 6. Iarc, 2004.

[29] Brian I Rini, Steven C Campbell, and Bernard Escudier. Renal cell carcinoma. *The Lancet*, 373(9669):1119–1132, 2009.

[30] John R Srigley and Brett Delahunt. Uncommon and recently described renal carcinomas. *Modern pathology*, 22:S2–S23, 2009.

[31] Sung-Im Do, Eduard Santini Araujo, Ricardo K Kalil, Patrizia Bacchini, Franco Bertoni, K Krishnan Unni, and Yong-Koo Park. Expression of embryonic lethal abnormal vision (elav)-like protein hur and cyclooxygenase-2 (cox-2) in ewing sarcoma. *Tumori*, 94(3):347, 2008.

[32] Wei-Jun Ma, Simon Cheng, Chris Campbell, Anne Wright, and Henry Furneaux. Cloning and characterization of hur, a ubiquitously expressed elav-like protein. *Journal of Biological Chemistry*, 271(14):8144–8151, 1996.

[33] Sabrina Danilin, Carole Sourbier, Lionel Thomas, Véronique Lindner, Sylvie Rothhut, Valérian Dormoy, Jean-Jacques Helwig, Didier Jacqmin, Hervé Lang, and Thierry Massfelder. Role of the rna-binding protein hur in human renal cell carcinoma. *Carcinogenesis*, 31(6):1018–1026, 2010.

[34] Mamata Singh. *Insights Into the Renal Protective Mechanisms of MRNA Binding Protein HuR*. PhD thesis, The Ohio State University, 2011.

[35] Min-Ju Kang, Byung-Kyu Ryu, Min-Goo Lee, Jikhyon Han, Jin-Hee Lee, Tae-Kyu Ha, Do-Sun Byun, Kwon-Seok Chae, Bong-Hee Lee, Hyang Sook Chun, et al. Nf-κb activates transcription of the rna-binding factor hur, via pi3k-akt signaling, to promote gastric tumorigenesis. *Gastroenterology*, 135(6):2030–2042, 2008.

[36] Suman Govindaraju and Beth S Lee. Adaptive and maladaptive expression of the mrna regulatory protein hur. *World journal of biological chemistry*, 4(4):111, 2013.

[37] Weijun Dai, Gen Zhang, and Eugene V Makeyev. Rna-binding protein hur autoregulates its expression by promoting alternative polyadenylation site usage. *Nucleic acids research*, 40(2):787–800, 2012.

[38] Virginie Dormoy-Raclet, Isabelle Ménard, Eveline Clair, Ghada Kurban, Rachid Mazroui, Sergio Di Marco, Christopher von Roretz, Arnim Pause, and Imed-Eddine Gallouzi. The rna-binding protein hur promotes cell migration and cell invasion by stabilizing the β-actin mrna in a u-rich-element-dependent manner. *Molecular and cellular biology*, 27(15):5365–5380, 2007.

[39] Natalia Filippova, Xiuhua Yang, Yimin Wang, G Yancey Gillespie, Cathy Langford, Peter H King, Crystal Wheeler, and L Burt Nabors. The rna-binding protein hur promotes glioma growth and treatment resistance. *Molecular Cancer Research*, 9(5):648–659, 2011.

[40] Isabel López de Silanes, Jinshui Fan, Xiaoling Yang, Alan B Zonderman, Olga Potapova, Ellen S Pizer, and Myriam Gorospe. Role of the rna-binding protein hur in colon carcinogenesis. *Oncogene*, 22(46):7146–7154, 2003.

[41] Mira Heinonen, Annabrita Hemmes, Kaisa Salmenkivi, Kotb Abdelmohsen, Suvi-Tuuli Vilén, Marko Laakso, Marjut Leidenius, Tuula Salo, Sampsa Hautaniemi, Myriam Gorospe, et al. Role of rna binding protein hur in ductal carcinoma in situ of the breast. *The Journal of pathology*, 224(4):529–539, 2011.

[42] Hiroaki Kitano. Computational systems biology. *Nature*, 420(6912):206–210, 2002.

[43] Yong Wang, Xiang-Sun Zhang, and Luonan Chen. Optimization meets systems biology. *BMC systems biology*, 4(Suppl 2):S1, 2010.

[44] Yong Wang, Xiang-Sun Zhang, and Luonan Chen. Computational systems biology: integration of sequence, structure, network, and dynamics. *BMC systems biology*, 5(Suppl 1):S1, 2011.

[45] Z Bibi, Jamil Ahmad, and UK Niazi. Dynamical modeling of the biological regulatory network of nf-kb activation in hiv-1. In *Computer Networks and Information Technology (ICCNIT), 2011 International Conference on*, pages 47–51. IEEE, 2011.

[46] René Thomas and Richard d'Ari. *Biological feedback*. CRC press, 1990.

[47] Erik Plahte, Thomas Mestl, and Stig W Omholt. Feedback loops, stability and multistationarity in dynamical systems. *Journal of Biological Systems*, 3(02):409–413, 1995.

[48] Rene Thomas. Regulatory networks seen as asynchronous automata: a logical description. *Journal of theoretical biology*, 153(1):1–23, 1991.

[49] René Thomas. Logical analysis of systems comprising feedback loops. *Journal of Theoretical Biology*, 73(4):631–656, 1978.

[50] Rene Thomas et al. Laws for the dynamics of regulatory networks. *International Journal of Developmental Biology*, 42:479–485, 1998.

[51] René Thomas, Denis Thieffry, and Marcelle Kaufman. Dynamical behaviour of biological regulatory networks i. biological role of feedback loops and practical use of the concept of the loop-characteristic state. *Bulletin of mathematical biology*, 57(2):247–276, 1995.

[52] Denis Thieffry and René Thomas. Dynamical behaviour of biological regulatory networks ii. immunity control in bacteriophage lambda. *Bulletin of Mathematical Biology*, 57(2):277–297, 1995.

[53] Zohra Khalis, Jean-Paul Comet, Adrien Richard, and Gilles Bernot. The smbionet method for discovering models of gene regulatory networks. *Genes, Genomes and Genomics*, 3(1):15–22, 2009.

[54] Adrien Richard. Smbionet-1.4 user manual. *a a*, 2(1):0, 2005.

[55] Hossam A Gabbar. *Modern formal methods and applications*. Springer Science & Business Media, 2006.

[56] Jan Lunze and Françoise Lamnabhi-Lagarrigue. *Handbook of hybrid systems control: theory, tools, applications*. Cambridge University Press, 2009.

[57] Jean-Paul Comet and Gilles Bernot. Introducing continuous time in discrete models of gene regulatory networks. *Proc. of the Nice Spring school on Modelling and simulation of biological processes in the context of genomics. EDP Sciences, ISBN*, pages 978–2, 2010.

[58] Thomas A Henzinger, Pei-Hsin Ho, and Howard Wong-Toi. Hytech: A model checker for hybrid systems. In *Computer aided verification*, pages 460–463. Springer, 1997.

[59] Jamil Ahmad, Olivier Roux, Gilles Bernot, and Jean-Paul Comet. Analysing formal models of genetic regulatory networks with delays. *International journal of bioinformatics research and applications*, 4(3):240–262, 2008.

[60] Babar Aslam, Jamil Ahmad, Amjad Ali, Rehan Zafar Paracha, Samar Hayat Khan Tareen, Umar Niazi, and Tariq Saeed. On the modelling and analysis of the regulatory network of dengue virus pathogenesis and clearance. *Computational biology and chemistry*, 53:277–291, 2014.

[61] Yuki Kuwano, Imed-Eddine Gallouzi, and Myriam Gorospe. Role of the rna-binding protein hur in apoptosis and apoptosome function. In *Apoptosome*, pages 203–220. Springer, 2010.

[62] Mototsugu Oya, Atsushi Takayanagi, Akio Horiguchi, Ryuichi Mizuno, Masafumi Ohtsubo, Ken Marumo, Nobuyoshi Shimizu, and Masaru Murai. Increased nuclear factor-κb activation is related to the tumor development of renal cell carcinoma. *Carcinogenesis*, 24(3):377–384, 2003.

[63] Daizo Oka, Kazuo Nishimura, Masahiro Shiba, Yasutomo Nakai, Yasuyuki Arai, Masashi Nakayama, Hitoshi Takayama, Hitoshi Inoue, Akihiko Okuyama, and Norio Nonomura. Sesquiterpene lactone parthenolide suppresses tumor growth in a xenograft model of renal cell carcinoma by inhibiting the activation of nf-κb. *International journal of cancer*, 120(12):2576–2581, 2007.

[64] Lingchong You. Toward computational systems biology. *Cell Biochemistry and Biophysics*, 40(2):167–184, 2004.

[65] Eric Alm and Adam P Arkin. Biological networks. *Current opinion in structural biology*, 13(2):193–202, 2003.

[66] Stefano Boccaletti, Vito Latora, and Yamir Moreno. *Handbook on biological networks*. World Scientific, 2010.

[67] Gilles Bernot, Franck Cassez, Jean-Paul Comet, Franck Delaplace, Céline Müller, and Olivier Roux. Semantics of biological regulatory networks. *Electronic Notes in Theoretical Computer Science*, 180(3):3–14, 2007.

[68] Alexandre Blais and Brian David Dynlacht. Constructing transcriptional regulatory networks. *Genes & development*, 19(13):1499–1511, 2005.

[69] Jamil Ahmad, Umar Niazi, Sajid Mansoor, Umair Siddique, and Jaclyn Bibby. Formal modeling and analysis of the mal-associated biological regulatory network: Insight into cerebral malaria. *PloS one*, 7(3):e33532, 2012.

[70] René Thomas and Marcelle Kaufman. Multistationarity, the basis of cell differentiation and memory. ii. logical analysis of regulatory networks in terms of feedback circuits. *Chaos: An Interdisciplinary Journal of Nonlinear Science*, 11(1):180–195, 2001.

[71] Gilles Bernot, Jean-Paul Comet, Adrien Richard, and Janine Guespin. Application of formal methods to biological regulatory networks: extending thomas asynchronous logical approach with temporal logic. *Journal of theoretical biology*, 229(3):339–347, 2004.

[72] Alessandro Cimatti, Edmund Clarke, Enrico Giunchiglia, Fausto Giunchiglia, Marco Pistore, Marco Roveri, Roberto Sebastiani, and Armando Tacchella.

Nusmv 2: An opensource tool for symbolic model checking. In *Computer Aided Verification*, pages 359–364. Springer, 2002.

[73] Alessandro Cimatti, Edmund Clarke, Fausto Giunchiglia, and Marco Roveri. Nusmv: A new symbolic model verifier. In *Computer Aided Verification*, pages 495–499. Springer, 1999.

[74] Alessandro Cimatti, Edmund Clarke, Fausto Giunchiglia, and Marco Roveri. Nusmv: a new symbolic model checker. *International Journal on Software Tools for Technology Transfer*, 2(4):410–425, 2000.

[75] Joshua O Madadhain, Danyel Fisher, Padhraic Smyth, Scott White, and Yan-Biao Boey. Analysis and visualization of network data using jung. *Journal of Statistical Software*, 10(2):1–35, 2005.

[76] Oliver Mason and Mark Verwoerd. Graph theory and networks in biology. *Systems Biology, IET*, 1(2):89–119, 2007.

[77] Michael Kohl, Sebastian Wiese, and Bettina Warscheid. Cytoscape: software for visualization and analysis of biological networks. In *Data Mining in Proteomics*, pages 291–303. Springer, 2011.

[78] Samar Hayat Khan Tareen. Formal analysis of the impact of feeding on hepatocyte circadian oscillators. Ms thesis, Research Centre for Modeling & Simulation (RCMS), National University of Sciences & Technology (NUST), Indus Loop, Sector H-12, Islamabad, 44000, Pakistan, August 2014.

[79] Ulrik Brandes and Thomas Erlebach. *Network analysis: methodological foundations*, volume 3418. Springer Science & Business Media, 2005.

[80] Réka Albert. Network inference, analysis, and modeling in systems biology. *The Plant Cell Online*, 19(11):3327–3338, 2007.

[81] Björn H Junker and Falk Schreiber. *Analysis of biological networks*, volume 2. John Wiley & Sons, 2011.

[82] Georgios A Pavlopoulos, Maria Secrier, Charalampos N Moschopoulos, Theodoros G Soldatos, Sophia Kossida, Jan Aerts, Reinhard Schneider, Pantelis G Bagos, et al. Using graph theory to analyze biological networks. *BioData mining*, 4(1):10, 2011.

[83] Michael S Branicky. Introduction to hybrid systems. In *Handbook of Networked and Embedded Control Systems*, pages 91–116. Springer, 2005.

[84] Assieh Saadatpour and Réka Albert. Boolean modeling of biological regulatory networks: a methodology tutorial. *Methods*, 62(1):3–12, 2013.

[85] Jamil Ahmad and Olivier Roux. Invariance kernel of biological regulatory networks. *International journal of data mining and bioinformatics*, 4(5):553–570, 2010.

[86] Jamil Ahmad, Gilles Bernot, Jean-Paul Comet, Didier Lime, and Olivier Roux. Hybrid modelling and dynamical analysis of gene regulatory networks with delays. *ComPlexUs*, 3(4):231–251, 2006.

[87] Christudas Morais, Glenda Gobe, David W Johnson, and Helen Healy. The emerging role of nuclear factor kappa b in renal cell carcinoma. *The international journal of biochemistry & cell biology*, 43(11):1537–1549, 2011.

Appendix

Appendix A

SMBioNet source files

Input file of HuR Associated BRN

```
VAR
AKT = 0 1;
NFKB = 0 1;
HuR = 0 1;
GRB10 = 0 1;

REG
AKT  [AKT >= 1]=> NFKB;
NFKB [NFKB >= 1]=> HuR;
HuR  [HuR >= 1]=> GRB10;
HuR  [HuR < 1]=> HuR;
GRB10 [GRB10 >= 1]=> AKT;

 PARA
 # Parameters for AKT
 K_AKT = 0  ;
 K_AKT+GRB10 =  1 ;

 # Parameters for NFKB
 K_NFKB = 0  ;
 K_NFKB+AKT =  1 ;

 # Parameters for HuR
 K_HuR = 0 1;
 K_HuR+HuR = 0 1 ;
 K_HuR+NFKB =  0 1 ;
```

```
 K_HuR+HuR+NFKB = 0 1 ;

 # Parameters for GRB10
 K_GRB10 = 0  ;
 K_GRB10+HuR =  1 ;

CTL
(AKT=1 & NFKB=0 & HuR=0 & GRB10=0)-> AX(EF(AKT=1 & NFKB=0 & HuR=0 & GRB10=0))
&
(AKT=1 & NFKB=0 & HuR=0 & GRB10=0)-> EF(AG(AKT=1 & NFKB=1 & HuR=1 & GRB10=1))
&
(AKT=1 & NFKB=0 & HuR=0 & GRB10=0)-> EF(AG(AKT=0 & NFKB=0 & HuR=0 & GRB10=0))
```

Output file of HuR Associated BRN

```
MODEL 1
 # K_AKT = 0
 # K_AKT+GRB10 = 1
 # K_NFKB = 0
 # K_NFKB+AKT = 1
 # K_HuR = 0
 # K_HuR+HuR = 0
 # K_HuR+NFKB = 0
 # K_HuR+HuR+NFKB = 0
 # K_GRB10 = 0
 # K_GRB10+HuR = 1

MODEL 2
 # K_AKT = 0
 # K_AKT+GRB10 = 1
 # K_NFKB = 0
 # K_NFKB+AKT = 1
 # K_HuR = 0
 # K_HuR+HuR = 0
 # K_HuR+NFKB = 0
 # K_HuR+HuR+NFKB = 1
 # K_GRB10 = 0
 # K_GRB10+HuR = 1

MODEL 3
 # K_AKT = 0
 # K_AKT+GRB10 = 1
```

```
 # K_NFKB = 0
 # K_NFKB+AKT = 1
 # K_HuR = 0
 # K_HuR+HuR = 1
 # K_HuR+NFKB = 0
 # K_HuR+HuR+NFKB = 1
 # K_GRB10 = 0
 # K_GRB10+HuR = 1

MODEL 4
 # K_AKT = 0
 # K_AKT+GRB10 = 1
 # K_NFKB = 0
 # K_NFKB+AKT = 1
 # K_HuR = 0
 # K_HuR+HuR = 0
 # K_HuR+NFKB = 1
 # K_HuR+HuR+NFKB = 1
 # K_GRB10 = 0
 # K_GRB10+HuR = 1

MODEL 5
 # K_AKT = 0
 # K_AKT+GRB10 = 1
 # K_NFKB = 0
 # K_NFKB+AKT = 1
 # K_HuR = 1
 # K_HuR+HuR = 1
 # K_HuR+NFKB = 1
 # K_HuR+HuR+NFKB = 1
 # K_GRB10 = 0
 # K_GRB10+HuR = 1
```

Appendix B

Table 1: 16 cycles obtained from the qualitative modeling of HuR associated pathway

CYCLES No	TRANSITIONS
Cycle No 1	[[0, 0, 0, 1] → [1, 0, 0, 1] → [1, 0, 0, 0] → [1, 1, 0, 0] → [0, 1, 0, 0] → [0, 1, 1, 0] → [0, 0, 1, 0] → [0, 0, 1, 1] → [0, 0, 0, 1]]
Cycle No 2	[[0, 0, 0, 1] → [1, 0, 0, 1] → [1, 0, 0, 0] → [1, 1, 0, 0] → [0, 1, 0, 0] → [0, 1, 1, 0] → [0, 1, 1, 1] → [0, 0, 1, 1] → [0, 0, 0, 1]]
Cycle No 3	[[0, 0, 0, 1] → [1, 0, 0, 1] → [1, 0, 0, 0] → [1, 1, 0, 0] → [1, 1, 1, 0] → [0, 1, 1, 0] → [0, 0, 1, 0] → [0, 0, 1, 1] → [0, 0, 0, 1]]
Cycle No 4	[[0, 0, 0, 1] → [1, 0, 0, 1] → [1, 0, 0, 0] → [1, 1, 0, 0] → [1, 1, 1, 0] → [0, 1, 1, 0] → [0, 1, 1, 1] → [0, 0, 1, 1] → [0, 0, 0, 1]]
Cycle No 5	[[0, 0, 1, 0] → [0, 0, 1, 1] → [1, 0, 1, 1] → [1, 0, 0, 1] → [1, 0, 0, 0] → [1, 1, 0, 0] → [0, 1, 0, 0] → [0, 1, 1, 0] → [0, 0, 1, 0]]
Cycle No 6	[[0, 0, 1, 0] → [0, 0, 1, 1] → [1, 0, 1, 1] → [1, 0, 0, 1] → [1, 0, 0, 0] → [1, 1, 0, 0] → [1, 1, 1, 0] → [0, 1, 1, 0] → [0, 0, 1, 0]]
Cycle No 7	[[0, 0, 1, 1] → [1, 0, 1, 1] → [1, 0, 0, 1] → [1, 0, 0, 0] → [1, 1, 0, 0] → [0, 1, 0, 0] → [0, 1, 1, 0] → [0, 1, 1, 1] → [0, 0, 1, 1]]
Cycle No 8	[[0, 0, 1, 1] → [1, 0, 1, 1] → [1, 0, 0, 1] → [1, 0, 0, 0] → [1, 1, 0, 0] → [1, 1, 1, 0] → [0, 1, 1, 0] → [0, 1, 1, 1] → [0, 0, 1, 1]]
Cycle No 9	[[0, 0, 0, 1] → [1, 0, 0, 1] → [1, 1, 0, 1] → [1, 1, 0, 0] → [0, 1, 0, 0] → [0, 1, 1, 0] → [0, 0, 1, 0] → [0, 0, 1, 1] → [0, 0, 0, 1]]
Cycle No 10	[[0, 0, 0, 1] → [1, 0, 0, 1] → [1, 1, 0, 1] → [1, 1, 0, 0] → [0, 1, 0, 0] → [0, 1, 1, 0] → [0, 1, 1, 1] → [0, 0, 1, 1] → [0, 0, 0, 1]]
Cycle No 11	[[0, 0, 0, 1] → [1, 0, 0, 1] → [1, 1, 0, 1] → [1, 1, 0, 0] → [1, 1, 1, 0] → [0, 1, 1, 0] → [0, 0, 1, 0] → [0, 0, 1, 1] → [0, 0, 0, 1]]
Cycle No 12	[[0, 0, 0, 1] → [1, 0, 0, 1] → [1, 1, 0, 1] → [1, 1, 0, 0] → [1, 1, 1, 0] → [0, 1, 1, 0] → [0, 1, 1, 1] → [0, 0, 1, 1] → [0, 0, 0, 1]]
Cycle No 13	[[0, 0, 1, 0] → [0, 0, 1, 1] → [1, 0, 1, 1] → [1, 0, 0, 1] → [1, 1, 0, 1] → [1, 1, 0, 0] → [0, 1, 0, 0] → [0, 1, 1, 0] → [0, 0, 1, 0]]
Cycle No 14	[[0, 0, 1, 0] → [0, 0, 1, 1] → [1, 0, 1, 1] → [1, 0, 0, 1] → [1, 1, 0, 1] → [1, 1, 0, 0] → [1, 1, 1, 0] → [0, 1, 1, 0] → [0, 0, 1, 0]]
Cycle No 15	[[0, 0, 1, 1] → [1, 0, 1, 1] → [1, 0, 0, 1] → [1, 1, 0, 1] → [1, 1, 0, 0] → [0, 1, 0, 0] → [0, 1, 1, 0] → [0, 1, 1, 1] → [0, 0, 1, 1]]
Cycle No 16	[[0, 0, 1, 1] → [1, 0, 1, 1] → [1, 0, 0, 1] → [1, 1, 0, 1] → [1, 1, 0, 0] → [1, 1, 1, 0] → [0, 1, 1, 0] → [0, 1, 1, 1] → [0, 0, 1, 1]]

Appendix C

HyTech Source Files

```
--Hytech file for cycle 1

 -- gene No0 = AKT
 -- gene No1 = NFKB
 -- gene No2 = HUR
 -- gene No3 = GRB10
 var
  dpAKT, dpNFKB, dnGRB10, dnHUR, dpGRB10, dnNFKB, dpHUR, dnAKT: parameter;
  hAKT , hNFKB, hHUR, hGRB10: analog;
  k,n: discrete;
  automaton auto
  synclabs: ;
  initially loc_1000;

 -- for the configuration 0,0,0,1
 loc loc_0001: while hAKT <= dpAKT wait{dhAKT=1,dhNFKB=1,dhHUR=0,dhGRB10=-1}
 when hAKT=dpAKT do {hAKT'=0, k'=k+1}} goto loc_1001;

 -- for the configuration 0,0,1,0
 loc loc_0010: while hGRB10 <= dpGRB10 wait {dhAKT=1,dhNFKB=0,dhHUR=-1,dhGRB10=1}
 when hGRB10=dpGRB10 do {hGRB10'=0, k'=k+1} goto loc_0011;

 -- for the configuration 0,0,1,1
 loc loc_0011: while hHUR >= dnHUR wait {dhAKT=1,dhNFKB=1,dhHUR=-1,dhGRB10=-1}
 when hHUR=dnHUR do {hHUR'=0, k'=k+1} goto loc_0001;

 -- for the configuration 0,1,0,0
 loc loc_0100: while hHUR <=dpHUR wait {dhAKT=0,dhNFKB=-1,dhHUR=1,dhGRB10=1}
 when hHUR=dpHUR do {hHUR'=0, k'=k+1} goto loc_0110;

 -- for the configuration 0,1,1,0
 loc loc_0110: while hNFKB >= dnNFKB wait {dhAKT=1,dhNFKB=-1,dhHUR=-1,dhGRB10=1}
 when hNFKB=dnNFKB do {hNFKB'=0, k'=k+1} goto loc_0010;

 -- for the configuration 1,0,0,0
 loc loc_1000:   while hNFKB <= dpNFKB wait {dhAKT=-1,dhNFKB=1,dhHUR=1,dhGRB10=0}
 when hNFKB=dpNFKB do {hNFKB'=0, k'=k+1} goto loc_1100;
```

```
-- for the configuration 1,0,0,1
loc loc_1001: while hNFKB <=dpNFKB wait{dhAKT=-1,dhNFKB=1,dhHUR=1,dhGRB10=-1}
when hGRB10=dnGRB10 do {hGRB10'=0, k'=k+1} goto loc_1000;

-- for the configuration 1,1,0,0
loc loc_1100: while hAKT >= dnAKT wait {dhAKT=-1,dhNFKB=-1,dhHUR=1,dhGRB10=1}
when hAKT=dnAKT do {hAKT'=0, k'=k+1} goto loc_0100;
end

--Analysis commands
var
portrait,fstate,nes_cyc_length,pln_cyc_length,fixpoint,r_ini,r_old,r_new,
r_acc: region;
r_ini:= loc[auto] = loc_1000  &  hNFKB>=0  &  hNFKB <=  dpNFKB;
r_new:=hide k,n in hull (post(r_ini  &  k=n)  &  ~k=n) endhide;
r_old:=r_ini  &  ~r_ini;
while not empty(r_new) and empty(r_new  &  r_ini) do
r_old:=r_new;
r_new:=hide k,n in hull(post(r_new  &  k=n)  &  ~k=n) endhide;
endwhile;
-- To verify that the initial zone is accessible from itself
if not empty (r_new & r_ini) then
r_acc:=hide k,n in hull(post(r_new & k=n) &~k=n) endhide;
r_old:=r_ini & ~r_ini; --empty region initialization
while not empty(r_acc) and not r_new<=r_old do
r_old:=r_new;
while not empty(r_acc) and empty(r_acc & r_ini) do
r_acc:= hide k,n in hull(post(r_acc & k=n) &~k=n) endhide;
endwhile;
r_acc:=hull(r_acc & r_ini);
r_new:=hull(r_acc & r_new);
r_acc:=hide k,n in hull(post(r_new & k=n) & ~k=n) endhide;
endwhile;
if not empty(r_new) then
 prints "================================";
prints " Delay constraintes: ";
print  hide hAKT,hNFKB,hHUR,hGRB10 in r_new endhide;
prints "================================";
else
prints "Invariance kernel does not exist from the initial region ";
endif;
else
```

```
 prints " The initial region is not accessible from itself hence " ;
 prints " There is no initial condition that leads to an invariance kernel.";
 endif;

--Hytech file for cycle 2

 -- gene No 0 = AKT
 -- gene No 1 = NFKB
 -- gene No 2 = HUR
 -- gene No 3 = GRB10
var
 dpAKT,dpNFKB,dnGRB10,dnHUR,dpGRB10,dnNFKB,dpHUR,dnAKT: parameter;
 hAKT,hNFKB,hHUR,hGRB10: analog;
 k,n: discrete;
 automaton auto
 synclabs: ;
 initially loc_1000;

 -- for the configuration 0,0,0,1
 loc loc_0001: while hAKT <= dpAKT wait{dhAKT=1,dhNFKB=1,dhHUR=0,dhGRB10=-1}
 when hAKT=dpAKT do {hAKT'=0, k'=k+1} goto loc_1001;

-- for the configuration 0,0,1,1
 loc loc_0011: while hHUR >= dnHUR wait{dhAKT=1,dhNFKB=1,dhHUR=-1,dhGRB10=-1}
 when hHUR=dnHUR do {hHUR'=0, k'=k+1} goto loc_0001;

 -- for the configuration 0,1,0,0
 loc loc_0100: while hHUR <= dpHUR wait{dhAKT=0,dhNFKB=-1,dhHUR=1,dhGRB10=1}
 when hHUR=dpHUR do {hHUR'=0, k'=k+1} goto loc_0110;

 -- for the configuration 0,1,1,0
 loc loc_0110: while hGRB10 <= dpGRB10 wait {dhAKT=1,dhNFKB=-1,dhHUR=-1,dhGRB10=1}
 when hGRB10=dpGRB10 do {hGRB10'=0, k'=k+1} goto loc_0111;

 -- for the configuration 0,1,1,1
 loc loc_0111: while hNFKB >= dnNFKB wait{dhAKT=1,dhNFKB=-1,dhHUR=-1,dhGRB10=0}
 when hNFKB=dnNFKB do {hNFKB'=0, k'=k+1} goto loc_0011;

 -- for the configuration 1,0,0,0
 loc loc_1000:  while hNFKB <= dpNFKB  wait {dhAKT=-1,dhNFKB=1,dhHUR=1,dhGRB10=0}
 when hNFKB=dpNFKB do {hNFKB'=0, k'=k+1} goto loc_1100;
```

```
 -- for the configuration 1,0,0,1
 loc loc_1001: while hGRB10 >= dnGRB10 wait {dhAKT=-1,dhNFKB=1,dhHUR=1,dhGRB10=-1}
 when hGRB10=dnGRB10 do {hGRB10'=0, k'=k+1} goto loc_1000;

 -- for the configuration 1,1,0,0
 loc loc_1100: while hAKT >= dnAKT wait {dhAKT=-1,dhNFKB=-1,dhHUR=1,dhGRB10=1}
 when hAKT=dnAKT do {hAKT'=0, k'=k+1} goto loc_0100;
end

 --Analysis commands
 var
 portrait,fstate,nes_cyc_length,pln_cyc_length,fixpoint,r_ini,r_old,r_new,
 r_acc: region;
 r_ini:= loc[auto] = loc_1000 & hNFKB>=0 & hNFKB <=  dpNFKB;
 r_new:=hide k,n in hull (post(r_ini & k=n) & ~k=n) endhide;
 r_old:=r_ini & ~r_ini;
 while not empty(r_new) and empty(r_new & r_ini) do
 r_old:=r_new;
 r_new:=hide k,n in hull(post(r_new & k=n) & ~k=n) endhide;
 endwhile;
 -- To verify that the initial zone is accessible from itself
 if not empty (r_new & r_ini) then
 r_acc:=hide k,n in hull(post(r_new & k=n) &~k=n) endhide;
 r_old:=r_ini & ~r_ini; --empty region initialization
 while not empty(r_acc) and not r_new<=r_old do
 r_old:=r_new;
 while not empty(r_acc) and empty(r_acc & r_ini) do
 r_acc:= hide k,n in hull(post(r_acc & k=n) &~k=n) endhide;
 endwhile;
 r_acc:=hull(r_acc & r_ini);
 r_new:=hull(r_acc & r_new);
 r_acc:=hide k,n in hull(post(r_new & k=n) & ~k=n) endhide;
 endwhile;
 if not empty(r_new) then
 prints "==================================";
 prints " Delay constraintes: ";
  print  hide hAKT,hNFKB,hHUR,hGRB10 in r_new endhide;
  prints "==================================";
 else
  prints "Invariance kernel does not exist from the initial region ";
 endif;
 else
```

```
prints " The initial region is not accessible from itself hence " ;
prints " there is no initial condition that leads to an invariance kernel.";
endif;

--Hytech file for cycle 3

-- gene No0 = AKT
-- gene No1 = NFKB
-- gene No2 = HUR
-- gene No3 = GRB10
var
dpAKT,dpNFKB,dnGRB10,dnHUR,dpGRB10,dnNFKB,dpHUR,dnAKT: parameter;
hAKT,hNFKB,hHUR,hGRB10: analog;
k,n: discrete;
automaton auto
synclabs: ;
initially loc_1000;

-- for the configuration 0,0,0,1
loc loc_0001: while hAKT <=dpAKT wait {dhAKT=1,dhNFKB=1,dhHUR=0,dhGRB10=-1}
when hAKT=dpAKT do {hAKT'=0, k'=k+1} goto loc_1001;

-- for the configuration 0,0,1,0
loc loc_0010: while hHUR >= dnHUR wait {dhAKT=1,dhNFKB=0,dhHUR=-1,dhGRB10=1}
when hGRB10=dpGRB10 do {hGRB10'=0, k'=k+1} goto loc_0011;

-- for the configuration 0,0,1,1
loc loc_0011:while hHUR >= dnHUR wait{dhAKT=1,dhNFKB=1,dhHUR=-1,dhGRB10=-1}
when hHUR=dnHUR do {hHUR'=0, k'=k+1} goto loc_0001;

-- for the configuration 0,1,1,0
loc loc_0110: while hNFKB >= dnNFKB wait {dhAKT=1,dhNFKB=-1,dhHUR=-1,dhGRB10=1}
when hNFKB=dnNFKB do {hNFKB'=0, k'=k+1} goto loc_0010;

-- for the configuration 1,0,0,0
loc loc_1000:while hNFKB <=dpNFKB wait{dhAKT=-1,dhNFKB=1,dhHUR=1,dhGRB10=0}
when hNFKB=dpNFKB do {hNFKB'=0, k'=k+1} goto loc_1100;

-- for the configuration 1,0,0,1
loc loc_1001:while hGRB10 >=dnGRB10 wait{dhAKT=-1,dhNFKB=1,dhHUR=1,dhGRB10=-1}
when hGRB10=dnGRB10 do {hGRB10'=0, k'=k+1} goto loc_1000;
```

```
 -- for the configuration 1,1,0,0
 loc loc_1100:while hHUR <=dpHUR wait{dhAKT=-1,dhNFKB=-1,dhHUR=1,dhGRB10=1}
 when hHUR=dpHUR do {hHUR'=0, k'=k+1} goto loc_1110;

 -- for the configuration 1,1,1,0
 loc loc_1110: while hGRB10 <= dpGRB10 wait {dhAKT=-1,dhNFKB=-1,dhHUR=0,dhGRB10=1}
 when hAKT=dnAKT do {hAKT'=0, k'=k+1} goto loc_0110;
 end

 --
Analysis commands
 var
 portrait,fstate,nes_cyc_length,pln_cyc_length,fixpoint,r_ini,r_old,r_new,
 r_acc: region;
 r_ini:= loc[auto] = loc_1000 & hNFKB>=0 & hNFKB <=  dpNFKB;
 r_new:=hide k,n in hull (post(r_ini & k=n) & ~k=n) endhide;
 r_old:=r_ini & ~r_ini;
 while not empty(r_new) and empty(r_new & r_ini) do
 r_old:=r_new;
 r_new:=hide k,n in hull(post(r_new & k=n) & ~k=n) endhide;
 endwhile;
 -- To verify that the initial zone is accessible from itself
 if not empty (r_new & r_ini) then
 ---- if accessible
 r_acc:=hide k,n in hull(post(r_new & k=n) &~k=n) endhide;
 r_old:=r_ini & ~r_ini; --empty region initialization
 while not empty(r_acc) and not r_new<=r_old do
 r_old:=r_new;
 while not empty(r_acc) and empty(r_acc & r_ini) do
 r_acc:= hide k,n in hull(post(r_acc & k=n) &~k=n) endhide;
 endwhile;
 r_acc:=hull(r_acc & r_ini);
 r_new:=hull(r_acc & r_new);
 r_acc:=hide k,n in hull(post(r_new & k=n) & ~k=n) endhide;
 endwhile;
 if not empty(r_new) then
  prints "================================";
  prints " Delay constraintes: ";
  print  hide hAKT,hNFKB,hHUR,hGRB10 in r_new endhide;
  prints "================================";
 else
  prints "Invariance kernel does not exist from the initial region ";
```

```
 endif;
 else
 prints " The initial region is not accessible from itself hence " ;
 prints " There is no initial condition that leads to an invariance kernel.";
 endif;

--Hytech file for cycle 4

 -- gene No0 = AKT
 -- gene No1 = NFKB
 -- gene No2 = HUR
 -- gene No3 = GRB10
var
 dpAKT,dpNFKB,dnGRB10,dnHUR,dpGRB10,dnNFKB,dpHUR,dnAKT: parameter;
 hAKT,hNFKB,hHUR,hGRB10: analog;
 k,n: discrete;
 automaton auto
 synclabs: ;
 initially loc_1000;

 -- for the configuration 0,0,0,1
 loc loc_0001: while hAKT <= dpAKT wait {dhAKT=1,dhNFKB=1,dhHUR=0,dhGRB10=-1}
 when hAKT=dpAKT do {hAKT'=0, k'=k+1} goto loc_1001;

 -- for the configuration 0,0,1,1
 loc loc_0011: while hHUR >= dnHUR wait {dhAKT=1,dhNFKB=1,dhHUR=-1,dhGRB10=-1}
 when hHUR=dnHUR do {hHUR'=0, k'=k+1} goto loc_0001;

 -- for the configuration 0,1,1,0
 loc loc_0110: while hGRB10 <= dpGRB10 wait {dhAKT=1,dhNFKB=-1,dhHUR=-1,dhGRB10=1}
 when hGRB10=dpGRB10 do {hGRB10'=0, k'=k+1} goto loc_0111;

 -- for the configuration 0,1,1,1
 loc loc_0111: while hNFKB >= dnNFKB wait {dhAKT=1,dhNFKB=-1,dhHUR=-1,dhGRB10=0}
 when hNFKB=dnNFKB do {hNFKB'=0, k'=k+1} goto loc_0011;

 -- for the configuration 1,0,0,0
 loc loc_1000: while hNFKB <= dpNFKB wait {dhAKT=-1,dhNFKB=1,dhHUR=1,dhGRB10=0}
 when hNFKB=dpNFKB do {hNFKB'=0, k'=k+1} goto loc_1100;

 -- for the configuration 1,0,0,1
 loc loc_1001: while hGRB10 >= dnGRB10 wait {dhAKT=-1,dhNFKB=1,dhHUR=1,dhGRB10=-1}
```

```
when hGRB10=dnGRB10 do {hGRB10'=0, k'=k+1} goto loc_1000;

-- for the configuration 1,1,0,0
loc loc_1100: while  hHUR <= dpHUR wait {dhAKT=-1,dhNFKB=-1,dhHUR=1,dhGRB10=1}
when hHUR=dpHUR do {hHUR'=0, k'=k+1} goto loc_1110;

-- for the configuration 1,1,1,0
loc loc_1110:  while hAKT >= dnAKT wait {dhAKT=-1,dhNFKB=-1,dhHUR=0,dhGRB10=1}
when hAKT=dnAKT do {hAKT'=0, k'=k+1} goto loc_0110;
end

--Analysis commands
var
portrait,fstate,nes_cyc_length,pln_cyc_length,fixpoint,r_ini,r_old,r_new,
r_acc: region;
r_ini:= loc[auto] = loc_1000 & hNFKB>=0 & hNFKB <=  dpNFKB;
r_new:=hide k,n in hull (post(r_ini & k=n) & ~k=n) endhide;
r_old:=r_ini & ~r_ini;
while not empty(r_new) and empty(r_new & r_ini) do
r_old:=r_new;
r_new:=hide k,n in hull(post(r_new & k=n) & ~k=n) endhide;
endwhile;
-- To verify that the initial zone is accessible from itself
if not empty (r_new & r_ini) then
---- if accessible
r_acc:=hide k,n in hull(post(r_new & k=n) &~k=n) endhide;
r_old:=r_ini & ~r_ini; --empty region initialization
while not empty(r_acc) and not r_new<=r_old do
r_old:=r_new;
while not empty(r_acc) and empty(r_acc & r_ini) do
r_acc:= hide k,n in hull(post(r_acc & k=n) &~k=n) endhide;
endwhile;
r_acc:=hull(r_acc & r_ini);
r_new:=hull(r_acc & r_new);
r_acc:=hide k,n in hull(post(r_new & k=n) & ~k=n) endhide;
endwhile;
if not empty(r_new) then
 prints "================================";
 prints " Delay constraintes: ";
 print  hide hAKT,hNFKB,hHUR,hGRB10 in r_new endhide;
 prints "================================";
else
```

```
 prints "Invariance kernel does not exist from the initial region ";
 endif;
 else
 prints " The initial region is not accessible from itself hence " ;
 prints " There is no initial condition that leads to an invariance kernel.";
 endif;

--Hytech file for cycle 5

 -- gene No0 = AKT
 -- gene No1 = NFKB
 -- gene No2 = HUR
 -- gene No3 = GRB10
 var
 dpAKT,dpNFKB,dnGRB10,dnHUR,dpGRB10,dnNFKB,dpHUR,dnAKT: parameter;
 hAKT,hNFKB,hHUR,hGRB10: analog;
 k,n,l: discrete;
 automaton auto
 synclabs: ;
 initially loc_1000;

 -- for the configuration 0,0,1,0
 loc loc_0010: while hGRB10 <= dpGRB10  wait {dhAKT=1,dhNFKB=0,dhHUR=-1,dhGRB10=1}
 when hGRB10=dpGRB10 do {hGRB10'=0, k'=k+1} goto loc_0011;

 -- for the configuration 0,0,1,1
 loc loc_0011: while hAKT <=  dpAKT wait {dhAKT=1,dhNFKB=1,dhHUR=-1,dhGRB10=-1}
 when hAKT=dpAKT do {hAKT'=0, k'=k+1} goto loc_1011;

 -- for the configuration 0,1,0,0
 loc loc_0100: while hHUR <= dpHUR wait {dhAKT=0,dhNFKB=-1,dhHUR=1,dhGRB10=1}
 when hHUR=dpHUR do {hHUR'=0, k'=k+1} goto loc_0110;

 -- for the configuration 0,1,1,0
 loc loc_0110: while hNFKB >= dnNFKB wait {dhAKT=1,dhNFKB=-1,dhHUR=-1,dhGRB10=1}
 when hNFKB=dnNFKB do {hNFKB'=0, k'=k+1} goto loc_0010;

 -- for the configuration 1,0,0,0
 loc loc_1000: while hNFKB <= dpNFKB wait {dhAKT=-1,dhNFKB=1,dhHUR=1,dhGRB10=0}
 when hNFKB=dpNFKB do {hNFKB'=0, k'=k+1} goto loc_1100;

 -- for the configuration 1,0,0,1
```

```
 loc loc_1001: while hGRB10 >=dnGRB10 wait {dhAKT=-1,dhNFKB=1,dhHUR=1,dhGRB10=-1}
 when hGRB10=dnGRB10 do {hGRB10'=0, k'=k+1} goto loc_1000;

 -- for the configuration 1,0,1,1
 loc loc_1011: while hHUR >= dnHUR wait {dhAKT=0,dhNFKB=1,dhHUR=-1,dhGRB10=-1}
 when hHUR=dnHUR do {hHUR'=0, k'=k+1} goto loc_1001;

 -- for the configuration 1,1,0,0
 loc loc_1100: while hAKT >= dnAKT wait {dhAKT=-1,dhNFKB=-1,dhHUR=1,dhGRB10=1}
 when hAKT=dnAKT do {hAKT'=0, k'=k+1} goto loc_0100;
end

 --Analysis commands
 var
 portrait,fstate,nes_cyc_length,pln_cyc_length,fixpoint,r_ini,r_old,r_new,
 r_acc: region;
 r_ini:= loc[auto] = loc_1000 & hNFKB>=0 & hNFKB <=  dpNFKB;
 r_new:=hide k,n in hull (post(r_ini & k=n) & ~k=n) endhide;
 r_old:=r_ini & ~r_ini;
 while not empty(r_new) and empty(r_new & r_ini) do
 r_old:=r_new;
 r_new:=hide k,n in hull(post(r_new & k=n) & ~k=n) endhide;
 endwhile;
 -- To verify that the initial zone is accessible from itself
 if not empty (r_new & r_ini) then
 ---- if accessible
 r_acc:=hide k,n in hull(post(r_new & k=n) &~k=n) endhide;
 r_old:=r_ini & ~r_ini; --empty region initialization
 while not empty(r_acc) and not r_new<=r_old do
 r_old:=r_new;
 while not empty(r_acc) and empty(r_acc & r_ini) do
 r_acc:= hide k,n in hull(post(r_acc & k=n) &~k=n) endhide;
 endwhile;
 r_acc:=hull(r_acc & r_ini);
 r_new:=hull(r_acc & r_new);
 r_acc:=hide k,n in hull(post(r_new & k=n) & ~k=n) endhide;
 endwhile;
 if not empty(r_new) then
  prints "================================";
  prints " Delay constraintes: ";
  print  hide hAKT,hNFKB,hHUR,hGRB10 in r_new endhide;
  prints "================================";
```

```
 else
  prints "Invariance kernel does not exist from the initial region ";
 endif;
 else
 prints " The initial region is not accessible from itself hence " ;
 prints " There is no initial condition that leads to an invariance kernel.";
 endif;

--Hytech file for cycle 6

 -- gene No0 = AKT
 -- gene No1 = NFKB
 -- gene No2 = HUR
 -- gene No3 = GRB10
var
 dpAKT,dpNFKB,dnGRB10,dnHUR,dpGRB10,dnNFKB,dpHUR,dnAKT: parameter;
 hAKT,hNFKB,hHUR,hGRB10: analog;
 k,n,l: discrete;
 automaton auto
 synclabs: ;
 initially loc_1000;

 -- for the configuration 0,0,1,0
 loc loc_0010: while hGRB10 <= dpGRB10 wait {dhAKT=1,dhNFKB=0,dhHUR=-1,dhGRB10=1}
 when hGRB10=dpGRB10 do {hGRB10'=0, k'=k+1} goto loc_0011;

 -- for the configuration 0,0,1,1
 loc loc_0011: while hAKT <= dpAKT wait {dhAKT=1,dhNFKB=1,dhHUR=-1,dhGRB10=-1}
 when hAKT=dpAKT do {hAKT'=0, k'=k+1} goto loc_1011;

 -- for the configuration 0,1,1,0
 loc loc_0110: while hNFKB >= dnNFKB wait {dhAKT=1,dhNFKB=-1,dhHUR=-1,dhGRB10=1}
 when hNFKB=dnNFKB do {hNFKB'=0, k'=k+1} goto loc_0010;

 -- for the configuration 1,0,0,0
 loc loc_1000: while hNFKB <= dpNFKB wait {dhAKT=-1,dhNFKB=1,dhHUR=1,dhGRB10=0}
 when hNFKB=dpNFKB do {hNFKB'=0, k'=k+1} goto loc_1100;

 -- for the configuration 1,0,0,1
 loc loc_1001: while hGRB10 >= dnGRB10 wait {dhAKT=-1,dhNFKB=1,dhHUR=1,dhGRB10=-1}
 when hGRB10=dnGRB10 do {hGRB10'=0, k'=k+1} goto loc_1000;
```

```
-- for the configuration 1,0,1,1
loc loc_1011: while hHUR >= dnHUR wait {dhAKT=0,dhNFKB=1,dhHUR=-1,dhGRB10=-1}
when hHUR=dnHUR do {hHUR'=0, k'=k+1} goto loc_1001;

-- for the configuration 1,1,0,0
loc loc_1100:  while hHUR <= dpHUR wait {dhAKT=-1,dhNFKB=-1,dhHUR=1,dhGRB10=1}
when hHUR=dpHUR do {hHUR'=0, k'=k+1} goto loc_1110;

-- for the configuration 1,1,1,0
loc loc_1110:  while hAKT >= dnAKT wait {dhAKT=-1,dhNFKB=-1,dhHUR=0,dhGRB10=1}
when hAKT=dnAKT do {hAKT'=0, k'=k+1} goto loc_0110;
end

--Analysis commands
var
portrait,fstate,nes_cyc_length,pln_cyc_length,fixpoint,r_ini,r_old,r_new,
r _acc: region;
r_ini:= loc[auto] = loc_1000 & hNFKB>=0 & hNFKB <=  dpNFKB;
r_new:=hide k,n in hull (post(r_ini & k=n) & ~k=n) endhide;
r_old:=r_ini & ~r_ini;
while not empty(r_new) and empty(r_new & r_ini) do
r_old:=r_new;
r_new:=hide k,n in hull(post(r_new & k=n) & ~k=n) endhide;
endwhile;
-- To verify that the initial zone is accessible from itself
if not empty (r_new & r_ini) then
---- if accessible
r_acc:=hide k,n in hull(post(r_new & k=n) &~k=n) endhide;
r_old:=r_ini & ~r_ini; --empty region initialization
while not empty(r_acc) and not r_new<=r_old do
r_old:=r_new;
while not empty(r_acc) and empty(r_acc & r_ini) do
r_acc:= hide k,n in hull(post(r_acc & k=n) &~k=n) endhide;
endwhile;
r_acc:=hull(r_acc & r_ini);
r_new:=hull(r_acc & r_new);
r_acc:=hide k,n in hull(post(r_new & k=n) & ~k=n) endhide;
endwhile;
if not empty(r_new) then
 prints "================================";
 prints " Delay constraintes: ";
 print  hide hAKT,hNFKB,hHUR,hGRB10 in r_new endhide;
```

```
 prints "================================";
 else
  prints "Invariance kernel does not exist from the initial region ";
 endif;
 else
 prints " The initial region is not accessible from itself hence " ;
 prints " There is no initial condition that leads to an invariance kernel.";
 endif;

--Hytech file for cycle 7

 -- gene No 0 = AKT
 -- gene No 1 = NFKB
 -- gene No 2 = HUR
 -- gene No 3 = GRB10
 var
 dpAKT,dpNFKB,dnGRB10,dnHUR,dpGRB10,dnNFKB,dpHUR,dnAKT: parameter;
 hAKT,hNFKB,hHUR,hGRB10: analog;
 k,n,l: discrete;
 automaton auto
 synclabs: ;
 initially loc_1000;

 -- for the configuration 0,0,1,1
 loc loc_0011: while hAKT <= dpAKT wait {dhAKT=1,dhNFKB=1,dhHUR=-1,dhGRB10=-1}
 when hAKT=dpAKT do {hAKT'=0, k'=k+1} goto loc_1011;

 -- for the configuration 0,1,0,0
 loc loc_0100: while hHUR <= dpHUR  wait {dhAKT=0,dhNFKB=-1,dhHUR=1,dhGRB10=1}
 when hHUR=dpHUR do {hHUR'=0, k'=k+1} goto loc_0110;

 -- for the configuration 0,1,1,0
 loc loc_0110: while hGRB10 <= dpGRB10 wait {dhAKT=1,dhNFKB=-1,dhHUR=-1,dhGRB10=1}
 when hGRB10=dpGRB10 do {hGRB10'=0, k'=k+1} goto loc_0111;

 -- for the configuration 0,1,1,1
 loc loc_0111: while hNFKB >= dnNFKB wait {dhAKT=1,dhNFKB=-1,dhHUR=-1,dhGRB10=0}
 when hNFKB=dnNFKB do {hNFKB'=0, k'=k+1} goto loc_0011;

 -- for the configuration 1,0,0,0
 loc loc_1000 : while hNFKB <= dpNFKB wait {dhAKT=-1,dhNFKB=1,dhHUR=1,dhGRB10=0}
 when hNFKB=dpNFKB do {hNFKB'=0, k'=k+1} goto loc_1100;
```

```
 -- for the configuration 1,0,0,1
 loc loc_1001: while hGRB10 >= dnGRB10 wait {dhAKT=-1,dhNFKB=1,dhHUR=1,dhGRB10=-1}
 when hGRB10=dnGRB10 do {hGRB10'=0, k'=k+1} goto loc_1000;

 -- for the configuration 1,0,1,1
 loc loc_1011: while hHUR >= dnHUR wait {dhAKT=0,dhNFKB=1,dhHUR=-1,dhGRB10=-1}
 when hHUR=dnHUR do {hHUR'=0, k'=k+1} goto loc_1001;

 -- for the configuration 1,1,0,0
 loc loc_1100: while hAKT >= dnAKT wait {dhAKT=-1,dhNFKB=-1,dhHUR=1,dhGRB10=1}
 when hAKT=dnAKT do {hAKT'=0, k'=k+1} goto loc_0100;
end

 --Analysis commands
 var
 portrait,fstate,nes_cyc_length,pln_cyc_length,fixpoint,r_ini,r_old,r_new,
 r _acc: region;
 r_ini:= loc[auto] = loc_1000 & hNFKB>=0 & hNFKB <=  dpNFKB;
 r_new:=hide k,n in hull (post(r_ini & k=n) & ~k=n) endhide;
 r_old:=r_ini & ~r_ini;
 while not empty(r_new) and empty(r_new & r_ini) do
 r_old:=r_new;
 r_new:=hide k,n in hull(post(r_new & k=n) & ~k=n) endhide;
 endwhile;
 -- To verify that the initial zone is accessible from itself
 if not empty (r_new & r_ini) then
 ---- if accessible
 r_acc:=hide k,n in hull(post(r_new & k=n) &~k=n) endhide;
 r_old:=r_ini & ~r_ini; --empty region initialization
 while not empty(r_acc) and not r_new<=r_old do
 r_old:=r_new;
 while not empty(r_acc) and empty(r_acc & r_ini) do
 r_acc:= hide k,n in hull(post(r_acc & k=n) &~k=n) endhide;
 endwhile;
 r_acc:=hull(r_acc & r_ini);
 r_new:=hull(r_acc & r_new);
 r_acc:=hide k,n in hull(post(r_new & k=n) & ~k=n) endhide;
 endwhile;
 if not empty(r_new) then
  prints "================================";
  prints " Delay constraintes: ";
```

```
  print  hide hAKT,hNFKB,hHUR,hGRB10 in r_new endhide;
  prints "================================";
 else
  prints "Invariance kernel does not exist from the initial region ";
 endif;
 else
 prints " The initial region is not accessible from itself hence " ;
 prints " There is no initial condition that leads to an invariance kernel.";
 endif;

--Hytech file for cycle 8

 -- gene No0 = AKT
 -- gene No1 = NFKB
 -- gene No2 = HUR
 -- gene No3 = GRB10
var
 dpAKT,dpNFKB,dnGRB10,dnHUR,dpGRB10,dnNFKB,dpHUR,dnAKT: parameter;
 hAKT,hNFKB,hHUR,hGRB10: analog;
 k,n,l: discrete;
 automaton auto
 synclabs: ;
 initially loc_1000;

 -- for the configuration 0,0,1,1
 loc loc_0011: while hAKT <= dpAKT wait {dhAKT=1,dhNFKB=1,dhHUR=-1,dhGRB10=-1}
 when hAKT=dpAKT do {hAKT'=0, k'=k+1} goto loc_1011;

 -- for the configuration 0,1,1,0
 loc loc_0110: while hGRB10 <= dpGRB10 wait {dhAKT=1,dhNFKB=-1,dhHUR=-1,dhGRB10=1}
 when hGRB10=dpGRB10 do {hGRB10'=0, k'=k+1} goto loc_0111;

 -- for the configuration 0,1,1,1
 loc loc_0111: while hNFKB >= dnNFKB wait {dhAKT=1,dhNFKB=-1,dhHUR=-1,dhGRB10=0}
 when hNFKB=dnNFKB do {hNFKB'=0, k'=k+1} goto loc_0011;

 -- for the configuration 1,0,0,0
 loc loc_1000: while hNFKB <= dpNFKB  wait {dhAKT=-1,dhNFKB=1,dhHUR=1,dhGRB10=0}
 when hNFKB=dpNFKB do {hNFKB'=0, k'=k+1} goto loc_1100;

 -- for the configuration 1,0,0,1
 loc loc_1001: while hGRB10 >= dnGRB10 wait {dhAKT=-1,dhNFKB=1,dhHUR=1,dhGRB10=-1}
```

```
 when hGRB10=dnGRB10 do {hGRB10'=0, k'=k+1} goto loc_1000;

 -- for the configuration 1,0,1,1
 loc loc_1011: while hHUR >=  dnHUR wait {dhAKT=0,dhNFKB=1,dhHUR=-1,dhGRB10=-1}
 when hHUR=dnHUR do {hHUR'=0, k'=k+1} goto loc_1001;

 -- for the configuration 1,1,0,0
 loc loc_1100: while hHUR <= dpHUR wait {dhAKT=-1,dhNFKB=-1,dhHUR=1,dhGRB10=1}
 when hHUR=dpHUR do {hHUR'=0, k'=k+1} goto loc_1110;

 -- for the configuration 1,1,1,0
 loc loc_1110: while hAKT >= dnAKT wait {dhAKT=-1,dhNFKB=-1,dhHUR=0,dhGRB10=1}
 when hAKT=dnAKT do {hAKT'=0, k'=k+1} goto loc_0110;
end
 --Analysis commands

 var
 portrait,fstate,nes_cyc_length,pln_cyc_length,fixpoint,r_ini,r_old,r_new,
 r _acc: region;
 r_ini:= loc[auto] = loc_1000 & hNFKB>=0 & hNFKB <=  dpNFKB;
 r_new:=hide k,n in hull (post(r_ini & k=n) & ~k=n) endhide;
 r_old:=r_ini & ~r_ini;
 while not empty(r_new) and empty(r_new & r_ini) do
 r_old:=r_new;
 r_new:=hide k,n in hull(post(r_new & k=n) & ~k=n) endhide;
 endwhile;
 -- To verify that the initial zone is accessible from itself
 if not empty (r_new & r_ini) then
 ---- if accessible
 r_acc:=hide k,n in hull(post(r_new & k=n) &~k=n) endhide;
 r_old:=r_ini & ~r_ini; --empty region initialization
 while not empty(r_acc) and not r_new=r_old do
 r_old:=r_new;
 while not empty(r_acc) and empty(r_acc & r_ini) do
 r_acc:= hide k,n in hull(post(r_acc & k=n) &~k=n) endhide;
 endwhile;
 r_acc:=hull(r_acc & r_ini);
 r_new:=hull(r_acc & r_new);
 r_acc:=hide k,n in hull(post(r_new & k=n) & ~k=n) endhide;
 prints " Delay constraintes: ";
  print  hide hAKT,hNFKB,hHUR,hGRB10 in r_new endhide;
  endwhile;
```

```
if not empty(r_new) then
 prints "================================";
 prints " Delay constraintes: ";
 print  hide hAKT,hNFKB,hHUR,hGRB10 in r_new endhide;
 prints "================================";
else
 prints "Invariance kernel does not exist from the initial region ";
endif;
else
prints " The initial region is not accessible from itself hence " ;
prints " There is no initial condition that leads to an invariance kernel.";
endif;
```